





UNIVERSITI  
TEKNOLOGI  
PETRONAS

# **Modeling and Simulation of Supersonic Natural Gas Dehydration using De Laval Nozzle**

**By**

**Wong Mee Kee**

**Dissertation submitted in partial fulfilment of  
the requirements for  
Bachelor of Engineering (Hons)  
(Chemical Engineering)**

**JULY 2009**

**Universiti Teknologi PETRONAS**

**Bandar Seri Iskandar**

**31750 Tronoh**

**Perak Darul Ridzuan**

**CERTIFICATION OF APPROVAL**

**Modeling and Simulation of Supersonic Natural Gas Dehydration**

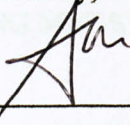
**Using De Laval Nozzle**

by

**Wong Mee Kee**

A project dissertation submitted to the  
Chemical Engineering Programme  
Universiti Teknologi PETRONAS  
in partial fulfilment of the requirement for the  
**BACHELOR OF ENGINEERING (Hons)**  
**(CHEMICAL ENGINEERING)**

Approved by,



\_\_\_\_\_  
(DR LAU KOK KEONG)

**UNIVERSITI TEKNOLOGI PETRONAS**

**TRONOH, PERAK**

**July 2009**

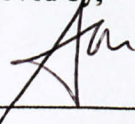
**CERTIFICATION OF APPROVAL**

**Modeling and Simulation of Supersonic Natural Gas Dehydration  
Using De Laval Nozzle  
by**

**Wong Mee Kee**

A project dissertation submitted to the  
Chemical Engineering Programme  
Universiti Teknologi PETRONAS  
in partial fulfilment of the requirement for the  
**BACHELOR OF ENGINEERING (Hons)**  
**(CHEMICAL ENGINEERING)**

Approved by,



\_\_\_\_\_  
(DR LAU KOK KEONG)

**UNIVERSITI TEKNOLOGI PETRONAS**

**TRONOH, PERAK**

**July 2009**



## CERTIFICATION OF ORIGINALITY

This is to certify that I am responsible for the work submitted in this project, that the original work is my own except as specified in the references and acknowledgements, and that the original work contained herein have not been undertaken or done by unspecified sources or persons.



---

WONG MEE KEE

## **ABSTRACT**

The purpose of this report is to provide an overview of the writer's Final Year Project. Current techniques in dehydration of natural gas, such as absorption, adsorption and membrane require relatively large facilities, a large investment, complex mechanical work, and the possibility of having a negative impact on the environment. Separation with supersonic flow is proposed as a solution to some of the disadvantages of conventional methods. The objectives of the project is to perform simulation which model natural gas flow through a convergent-divergent nozzle which separates water from natural gas and study pressure and temperature drop as well as the effectiveness of the separation. FLUENT and GAMBIT are the major tool used in running the simulation. Simple explanation on the methods is provided in this report.

Gas is accelerated up to velocities exceeding the sound propagation velocity in gas through a convergent-divergent nozzle due to transformation of a part of the potential energy of flow to kinetic energy the gas is cooled greatly. The result of the simulation shows velocity of gas increases significantly at the choke, resulting in temperature drop which condenses water vapour in the gas mixture. By removing water liquid droplets, water content in system can be reduced. Temperature, pressure, velocity and component mass fraction profiles are included in the report. Furthermore, effects of different inlet mass flow rate are studied. Higher inlet mass flow rate increases temperature drop, hence more water vapour is condensed and lower water content left in natural gas. For effective separation, sufficient inlet mass flow rate is required to achieve sonic flow in a 3-inch pipeline. Recommendations for future work expansion and continuation are provided at the end of the report.

## **ACKNOWLEDGEMENT**

The author would like to thank her supervisor, Dr Lau Kok Keong for his guidance and support throughout FYP I and II despite his many other obligations. Appreciation is also extended to the course coordinator, Dr Khalik B Mohd Sabil for his timely arrangement and valuable advices. Special thanks go to her family members and fellow friends who gave moral support to motivate her to pursue to greater heights in the project. Genuine gratitude is dedicated to examiners and evaluators, both internal and external.



## TABLE OF CONTENTS

<b>ABSTRACT .....</b>	<b>i</b>
<b>ACKNOWLEDGEMENT .....</b>	<b>ii</b>
<b>LIST OF FIGURES .....</b>	<b>v</b>
<b>LIST OF TABLES .....</b>	<b>vi</b>
<b>CHAPTER 1: INTRODUCTION .....</b>	<b>1</b>
1.1 Background of study .....	1
1.2 Problem statement .....	2
1.3 Objectives of project .....	2
1.4 Scope of study .....	3
<b>CHAPTER 2: LITERATURE REVIEW .....</b>	<b>4</b>
2.1 Dehydration Methods .....	4
2.1.1 Absorption of Water in Glycols .....	4
2.1.2 Adsorption of Water by a Solid .....	5
2.1.3 Membrane separation .....	6
2.1.4 Refrigeration .....	7
2.2 Hydrocarbon dew point .....	7
2.3 Joule-Thomson effect .....	8
2.4 Supersonic flow .....	9
2.5 Nozzle system design .....	10
2.6 Supersonic gas technology .....	12
2.6.1 3S supersonic gas separation technique .....	12
2.6.2 TWISTER supersonic separator .....	13
<b>CHAPTER 3: METHODOLOGY .....</b>	<b>15</b>
<b>CHAPTER 4 RESULT AND DISCUSSION .....</b>	<b>16</b>
4.1 2D Modeling and Simulation .....	16
4.1.1 Gambit Drawing .....	16
4.1.2 Fluid flow simulation .....	16
4.1.3 Effects of different inlet mass flow rate .....	22
4.2 3D Modeling and Simulation .....	27
4.2.1 Gambit Drawing .....	27
4.2.2 Fluid flow simulation .....	28
4.2.3 Summary of Simulation .....	39
4.3 Validation of Simulation Result .....	43

<b>CHAPTER 5 CONCLUSION AND RECOMMENDATIONS .....</b>	<b>44</b>
<b>5.1 Conclusion .....</b>	<b>44</b>
<b>5.2 Recommendations .....</b>	<b>45</b>
<b>REFERENCES.....</b>	<b>46</b>
<b>APPENDICES</b>	
<b>APPENDIX A: Gantt Charts</b>	
<b>APPENDIX B: Simulation Results</b>	
<b>APPENDIX C: Simulation Model Validation Data</b>	



## LIST OF FIGURES

Figure 1: Hydrocarbon and Water Dew Point Variation with Pressure for a Typical Natural Gas Composition.....	8
Figure 2: Graph of flow velocity, temperature and pressure proportional with the flow across nozzle. ....	11
Figure 3: Schematic diagram of 3S supersonic gas separator.....	12
Figure 4: Twister supersonic separator.....	13
Figure 5: Project Flow Chart.....	15
Figure 6: Gambit 2D drawing of convergent-divergent nozzle (unit in meter).....	16
Figure 7: Velocity profile in unit m/s .....	17
Figure 8: Velocity distribution along x-direction .....	17
Figure 9: Temperature profile in unit Kelvin.....	18
Figure 10: Temperature distribution along x-direction.....	18
Figure 11: Pressure profile in unit Pascal .....	19
Figure 12: Pressure distribution along x-direction.....	19
Figure 13: Mass fraction of water vapour.....	20
Figure 14: Mass fraction of methane .....	21
Figure 15: Mass fraction of carbon dioxide .....	21
Figure 16: Mass fraction of hydrogen sulphide .....	22
Figure 17: Velocity profile in unit m/s at inlet mass flow rate of 180kg/s .....	23
Figure 18: Temperature profile in unit Kelvin at inlet mass flow rate of 180kg/s .....	23
Figure 19: Mass fraction of water vapour at inlet mass flow rate of 180kg/s .....	24
Figure 20: Velocity profile in unit m/s at inlet mass flow rate of 100kg/s .....	25
Figure 21: Temperature profile in unit Kelvin at inlet mass flow rate of 100kg/s .....	25
Figure 22: Mass fraction of water vapor at inlet mass flow rate of 100kg/s .....	26
Figure 23: Mass fraction of methane at inlet mass flow rate of 100kg/s.....	26
Figure 24: Gambit 3D drawing of convergent-divergent nozzle (unit in meter).....	27
Figure 25: Static pressure profile at inlet mass flow rate of 4kg/s.....	29
Figure 26: Static pressure distribution along x-axis at inlet mass flow rate of 4kg/s .....	29
Figure 27: Velocity profile at inlet mass flow rate of 4kg/s .....	30

Figure 28: Velocity distribution along x-axis at inlet mass flow rate of 4kg/s.....	30
Figure 29: Mach number at inlet mass flow rate of 4kg/s .....	31
Figure 30: Temperature profile at inlet mass flow rate of 4kg/s.....	31
Figure 31: Temperature distribution along x-axis at inlet mass flow rate of 4kg/s .....	32
Figure 32: Molar concentration profile of water vapor at inlet mass flow rate of 4kg/s ..	32
Figure 33: Molar concentration distribution of water vapor along x-axis at inlet mass flow rate of 4kg/s.....	33
Figure 34: Static pressure profile at inlet mass flow rate of 5kg/s.....	34
Figure 35: Pressure distribution along x-axis at inlet mass flow rate of 5kg/s .....	34
Figure 36: Temperature profile at inlet mass flow rate of 5kg/s.....	35
Figure 37: Temperature distribution along x-axis at inlet mass flow rate of 5kg/s .....	35
Figure 38: Velocity profile at inlet mass flow rate of 5kg/s .....	36
Figure 39: Velocity distribution along x-axis at inlet mass flow rate of 5kg/s.....	36
Figure 40: Mach number at inlet mass flow rate of 5kg/s .....	37
Figure 41: Molar concentration profile of water vapor at inlet mass flow rate of 5kg/s ..	37
Figure 42: Molar concentration of water vapor along x-axis at inlet mass flow rate of 5kg/s .....	38
Figure 43: Pressure at choke and temperature at different velocities .....	39
Figure 44: Water removed at different inlet mass flow rates.....	41
Figure 45: Outlet mass percent of water vapour at different inlet mass flow rates .....	42
Figure 46: Outlet mass fraction at different inlet mass flow rates .....	42

## **LIST OF TABLES**

<b>Table 1: Simulation inputs</b>	<b>28</b>
<b>Table 2: Pressure drop, pressure at throat, temperature drop and water removed</b>	<b>40</b>



## CHAPTER 1: INTRODUCTION

### 1.1 Background of study

Natural gas extracted from underground sources is saturated with liquid water and heavier molecular weight hydrocarbon components. In order to meet the requirements for a clean, dry, wholly gaseous fuel suitable for transmission through pipelines and distribution for burning by end users, the gas must go through several stages of processing, including drying to reduce water vapour content. The dehydration of natural gas is critical to the successful operation of the production facility and the whole distribution train through to the end user. The presence of water vapour in concentrations above a few 10s of parts per million has potentially disastrous consequences. From the gas quality perspective, water is a common impurity in natural gas streams, and removal of it is necessary because water vapor becomes liquid water under low temperature and/or high-pressure conditions.

The lifetime of a pipeline is governed by the rate at which corrosion occurs which is directly linked to the available moisture in the gas which promotes oxidation, particularly when carbon dioxide and hydrogen sulfide are present in the gas. In addition, the formation of hydrates can reduce pipeline flow capacities, even leading to blockages, and potential damage to process filters, valves and compressors. Such hydrates are the combination of excessive water vapour with liquid hydrocarbons, which may condense out of the gas in the course of transmission, to form emulsions that, under process pressure conditions, are solid masses. Besides, liquid water in a natural gas pipeline potentially causes slugging flow conditions resulting in lower flow efficiency of the pipeline. Moreover, water content decreases the heating value of natural gas being transported.

## **1.2 Problem statement**

The dwindling high quality crude oil reserves and increasing demand for natural gas has encouraged energy industries further towards the discovery of remote offshore reservoirs. Consequently, new technologies have to be developed to efficiently produce and transport stranded natural gas to consuming markets. Compactness of production systems is the most challenging design criteria for offshore applications. Current separation techniques used in dehydration of natural gas are absorption, adsorption, membrane and refrigeration. Setbacks of these methods are they require relatively large facilities, a considerable investment, complex mechanical work, and the possibility of having a negative impact on the environment. Supersonic gas processing system is able to overcome some of the disadvantages of the conventional processes for dehydration.

## **1.3 Objectives of project**

The objectives of the project are to:

- incorporate mathematical model into Computational Fluid Dynamic
- simulate natural gas flow through De Lava nozzle and study the effectiveness of water separation from supersonic gas flow
- determine system temperature and pressure drop due to sudden expansion after going through the throttling process as well as composition of components throughout the system



## 1.4 Scope of study

The case studies are mainly about cooling and condensation of water vapour in natural gas. Study of thermodynamic and fluid flow of the gas mixture through a system consists of a convergent-divergent nozzle which accelerates gas flow, generates supersonic flow and creates cooling effect. 2D and 3D simulation are performed to model the fluid flow through throttling effect. Temperature, pressure and composition changes throughout the system are observed and analyzed to determine the effectiveness of the water removal technique.

As natural gas composes mainly of methane, the rest of the other hydrocarbons usually present are disregarded. Meaning the other light gases such as ethane, propane and so on, is not in the scope of study, to reduce the complexity involved when dealing with FLUENT. However, non-hydrocarbons species,  $\text{CO}_2$  and  $\text{H}_2\text{S}$  are given due attention as they are considered substantial water-content contributors besides hydrocarbon.

The project involves finding out operating conditions best for separation of liquid from the gas system. Therefore, it will be advantageous to acknowledge the typical pressure and temperature in the gas pipeline and in the associated processing plant. Kolass states that in on-shore transmission (gas entering offshore pipelines) is often compressed to 16 MPa (160 bar) or higher and in processing plant, the pressure of natural gas is typically 4 MPa (40 bar) to 8 MPa (80 bar). A typical sour natural gas project example by Kolass specifies the maximum permissible moisture content to be at 50 mgH<sub>2</sub>O/std.m<sup>3</sup>.

In this project the water vapour content in the vapour outlet of the separator device is set to be at 0.00014 mole fraction, equivalent to approximately 7 lb/MMscf. The range of pressure is set to be 60 bar (860 psi) to 245 bar (3,600 psi) which cover well the range of pressure in the pipeline and in processing plant. The temperature of study is from 40 °F to 140°F (4.5 °C – 60 °C), which also cover well the operating regime of a gas pipeline. The temperature is neither too low nor too high because the design of the separator device shall strive to minimize the need for coolant and heating medium to achieve separation.

## CHAPTER 2: LITERATURE REVIEW

### 2.1 Dehydration Methods

Removal of water from natural gas and can be accomplished by several alternative methods, which are discussed in the following part.

#### 2.1.1 Absorption of Water in Glycols

Absorption dehydration involves the use of a liquid desiccant to remove water vapor from the gas. The glycols, particularly ethylene glycol (EG), diethylene glycol (DEG), triethylene glycol (TEG), and tetraethylene glycol (T4EG) have chemical affinity for water and removes water from the gas stream. Water and the glycols show complete mutual solubility in the liquid phase due to hydrogen-oxygen bonds, and their water vapor pressures are very low. In this process, DEG or TEG is brought into contact with the wet gas stream in a *contactor*. The glycol solution absorbs water from the wet gas and, once absorbed, the glycol particles become heavier and sink to the bottom of the contactor where they are removed. The natural gas, having been stripped of most of its water content, is then transported out of the dehydrator.

Water may be removed from gas streams at the same time as hydrogen sulfide is removed. A widely used dehydration and desulfurization process is the glycolamine process, in which the treatment solution is a mixture of ethanolamine and a large amount of glycol. The mixture is circulated through an absorber and a reactivator. The glycol absorbs moisture from the hydrocarbon gas passing up the absorber; the ethanolamine absorbs hydrogen sulfide and carbon dioxide. The treated gas leaves the top of the absorber; the spent ethanolamineglycol mixture enters the reactivator tower, where heat drives off the absorbed acid gases and water. This technology needs a large facility and due to the need for glycol, there is a possibility for some operational problems such as corrosion, foaming in contactor device, fouling of heat transfer surfaces, glycol contamination and loss.



### 2.1.2 Adsorption of Water by a Solid

Adsorption (or solid bed) dehydration is the process where a solid desiccant is used for the removal of water vapor from a gas stream. The solid desiccants commonly used for gas dehydration are those that can be regenerated and, consequently, used over several adsorption-desorption cycles.

#### i. Alumina

A hydrated form of aluminum oxide ( $\text{Al}_2\text{O}_3$ ), alumina is the least expensive adsorbent. It is activated by driving off some of the water associated with it in its hydrated form ( $(\text{Al}_2\text{O}_3 \cdot 3\text{H}_2\text{O})$ ) by heating. It produces an excellent dew point depression values as low as  $-100^\circ\text{F}$ , but requires much more heat for regeneration.

Also, it is alkaline and cannot be used in the presence of acid gases, or acidic chemicals used for well treating. The tendency to adsorb heavy hydrocarbons is high, and it is difficult to remove these during regeneration. It has good resistance to liquids, but little resistance to disintegration due to mechanical agitation by the flowing gas.

#### ii. Calcium chloride

Solid anhydrous ( $\text{CaCl}_2$ ) which forms various  $\text{CaCl}_2$  hydrates when combined with water can be also used as desiccant to dehydrate natural gas. As water absorption continues, brine solution will be formed. In this unit calcium chloride pellets are placed in a fixed bed. The units might show poor performance under some conditions if  $\text{CaCl}_2$  pellets bond together and form a solid bridge in the tower. These units produce a waste stream that has to be taken care of appropriately

#### iii. Silica gel and silica-alumina gel

Gels are granular, amorphous solids manufactured by chemical reaction. Gels manufactured from sulfuric acid and sodium silicate reaction are called silica gels, and consist almost solely of silicon dioxide ( $\text{SiO}_2$ ). Alumina gels consist primarily of some hydrated form of  $\text{Al}_2\text{O}_3$ . Silica-alumina gels are a combination of silica

and alumina gel. Gels can dehydrate gas to as low as 10 ppm, and have the greatest ease of regeneration of all desiccants.

They adsorb heavy hydrocarbons, but release them relatively more easily during regeneration. Since they are acidic, they can handle sour gases, but not alkaline materials such as caustic or ammonia. Although there is no reaction with H<sub>2</sub>S, sulfur can deposit and block their surface. Therefore, gels are useful if the H<sub>2</sub>S content is less than 5-6%.

#### **iv. Molecular Sieves**

These are a crystalline form of alkali metal (calcium or sodium) alumina-silicates. They are highly porous, with a very narrow range of pore sizes, and very high surface area. Manufactured by ion-exchange, molecular sieves are the most expensive adsorbents. They possess highly localized polar charges on their surface that act as extremely effective adsorption sites for polar compounds such as water and hydrogen sulfide. Molecular sieves are alkaline and subject to attack by acids. Special acid-resistant sieves are available for very sour gases.

Since the pore size range is narrow, molecular sieves exhibit selectivity towards adsorbates on the basis of their molecular size, and tend not to adsorb bigger molecules such as the heavy hydrocarbons. The regeneration temperature is very high. They can produce water content as low as 1 ppm. Molecular sieves offer a means of simultaneous dehydration and desulfurization and are therefore the best choice for sour gases.

### **2.1.3 Membrane separation**

Membranes have been successfully used to remove acid gases from natural gas. They have also been successfully used for dehydration of air. They are also being promoted by suppliers of membrane technologies for water removal. They are relatively expensive (especially for large gas flow rates) and can be easily fouled by gas contaminants. They also need high pressure for efficient operation. However, they have a low-pressure drop



through the process and do not need any chemical reagents. The installation and change of the membrane cartridges are relatively easy and the maintenance cost is low. The membranes' capability to remove water vapour is not selective and part of the gas is always wasted through co-permeation.

#### **2.1.4 Refrigeration**

The simplest method of water removal is to cool the gas to a temperature at least equal to or below the dew point by refrigeration or cryogenic separation. The saturated vapor content of natural gas decreases with increased pressure or decreased temperature. Thus, hot gases saturated with water may be partially dehydrated by direct cooling. Gases subjected to compression are normally "after cooled", and this cooling may well remove water from the gas. The cooling process must reduce the temperature to the lowest value that the gas will encounter at the prevailing pressure to prevent further condensation of water. In most cases, cooling alone is insufficient for use in field operations.

#### **2.2 Hydrocarbon dew point**

For natural gas there are two dew-point temperatures of relevance, the water dew point, and the hydrocarbon dewpoint. The latter is quite simply the temperature at which liquid hydrocarbons condense out of the gas upon cooling. Such liquid hydrocarbons comprise the heavier molecular weight components of the gas composition, typically butane and higher. This parameter, as with water dew point, requires dedicated processing plant (in the form of condensing chillers) and purpose designed measurement instrumentation.



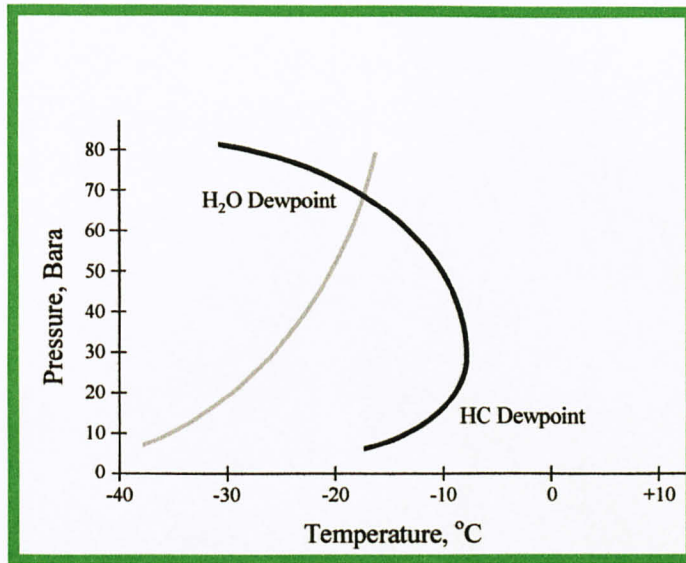


Figure 1: Hydrocarbon and Water Dew Point Variation with Pressure for a Typical Natural Gas Composition

### 2.3 Joule-Thomson effect

As a gas expands, the average distance between molecules grows. Because of intermolecular attractive forces, expansion causes an increase in the potential energy of the gas. If no external work is extracted in the process and no heat is transferred, the total energy of the gas remains the same because of the conservation of energy. The increase in potential energy thus implies a decrease in kinetic energy and therefore in temperature. Due to the sudden pressure and temperature drop, water vapour condenses and falls out of the stream as liquid droplet while pure methane gas stream continues to flow.

In thermodynamics, the Joule-Thomson effect, describes the temperature changes of a gas or liquid when it is forced through a valve or porous plug while being insulated so that no heat is lost to the environment. This procedure is called throttling process or Joule Thomson process. At room temperature, all gases except hydrogen, helium and neon cool upon expansion by Joule Thomson process.

In practice, the Joule–Thomson effect is achieved by allowing the gas to expand through a throttling device (usually a valve) which must be very well insulated to prevent any heat transfer to or from the gas. No external work is extracted from the gas during the expansion. Only when the Joule–Thomson coefficient for the given gas at the given temperature is greater than zero can the gas be liquefied at that temperature by the Linde cycle. In other words, a gas must be below its inversion temperature to be liquefied by the Linde cycle.

Joule–Thomson cooling occurs when a non-ideal gas expands from high to low pressure at constant enthalpy. The effect can be amplified by using the cooled gas to pre-cool the incoming gas in a heat exchanger.

## **2.4 Supersonic flow**

The term supersonic is used to define a speed that is over the speed of sound (Mach 1). In methane, the value required for an object to be travelling at a supersonic speed is approximately 460 m/s. Supersonic flow behaves very differently from subsonic flow. Fluids react to differences in pressure; pressure changes are how a fluid is "told" to respond to its environment. Therefore, since sound is in fact an infinitesimal pressure difference propagating through a fluid, the speed of sound in that fluid can be considered the fastest speed that "information" can travel in the flow. This difference most obviously manifests itself in the case of a fluid striking an object. In front of that object, the fluid builds up a stagnation pressure as impact with the object brings the moving fluid to rest. In fluid travelling at subsonic speed, this pressure disturbance can propagate upstream, changing the flow pattern ahead of the object and giving the impression that the fluid "knows" the object is there and is avoiding it. However, in a supersonic flow, the pressure disturbance cannot propagate upstream. Thus, when the fluid finally does strike the object, it is forced to change its properties, such as temperature, density, pressure, and Mach number in an extremely violent and irreversible fashion called a shock wave.



## 2.5 Nozzle system design

To design a nozzle that efficiently converting the energy of high pressure gas to kinetic energy, the nozzle should be composed of three sections, namely the converging section, throat and diverging section. The function of the converging part is to keep the flow uniform and parallel as well as to accelerate the gas. The gas flow through a de Laval nozzle is isentropic (gas entropy is nearly constant). At subsonic flow the gas is compressible; sound, a small pressure wave, will propagate through it. Within the converging section leading to the throat area, the gas is accelerated because of the constant mass flow rate so that sonic is reached at the throat and the converging curvature keeps the velocity of the flow uniform. At the throat, where the cross sectional area is a minimum, the gas velocity locally becomes sonic (Mach number = 1.0), a condition called choked flow. As the nozzle cross sectional area increases the gas begins to expand and the gas flow increases to supersonic velocities where a sound wave will not propagate backwards through the gas as viewed in the frame of reference of the nozzle.

The nozzle will only choke at the throat if the pressure and mass flow through the nozzle is sufficient to reach sonic speeds. In addition, the pressure of the gas at the exit of the expansion portion of the exhaust of a nozzle must not be too low. Because pressure cannot travel upstream through the supersonic flow, the exit pressure can be significantly below ambient pressure it exhausts into, but if it is too far below ambient, the flow will cease to be supersonic, or the flow will separate within the expansion portion of the nozzle, forming an unstable jet that may flop around within the nozzle, possibly damaging it. In practice ambient pressure must be no higher than roughly 2-3 times the pressure in the supersonic gas at the exit for supersonic flow to leave the nozzle.

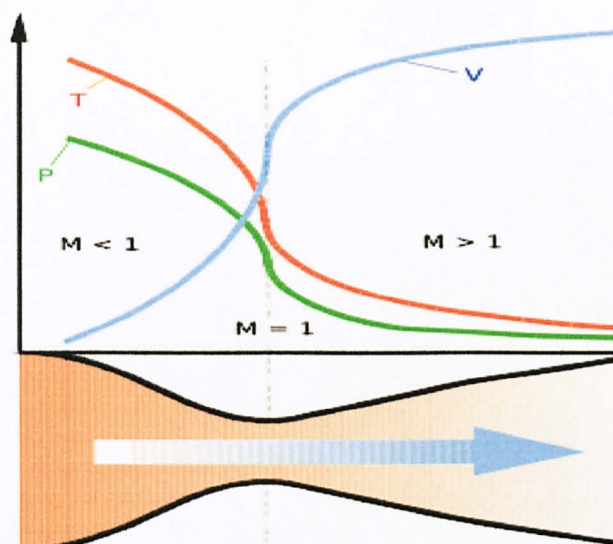


Figure 2: Graph of flow velocity, temperature and pressure proportional with the flow across nozzle.

Figure 2 shows the result of velocity, temperature and pressure proportion with the flow throughout the nozzle. Sudden expansion after the throat causes the temperature and pressure to drop significantly which causes condensation of water vapor. The velocity of the supersonic flow will increase after passes through the throat. Mach number at the throat is ideally equal to 1 while the Mach number after the throat will be larger than 1.

When the sonic flow is reached at the throat, the diverging part can further accelerate the flow depending on the outlet condition. This causes a fall in pressure and temperature as well as increase in gas velocity. It is likely that under certain condition, the flow cannot expand isentropically to the exit pressure, therefore an irreversible discontinuity, called normal shock can occur. During this process, large change in pressure and temperature can occur in a small distance.



## 2.6 Supersonic gas technology

### 2.6.1 3S supersonic gas separation technique

A new group of technologies has been developed for the separation and processing of natural gas components based on the adiabatic cooling of swirling gas flow in a supersonic nozzle. In September, 2004, a complex consisting of two “3S” facilities with a capacity of above 400 mmscm per year each was successfully put into pilot production operation at one of the gas treatment plants in Western Siberia as a part of the LPG complex.

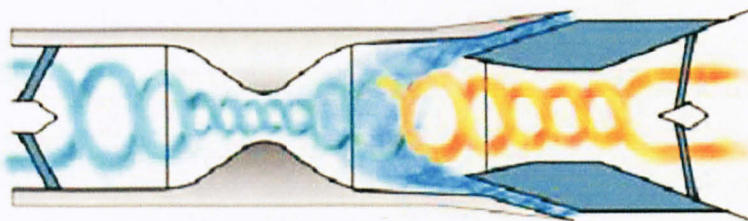


Figure 3: Schematic diagram of 3S supersonic gas separator

The mixed Hydrocarbon Stream enters the 3S unit as pictured from the left. Flowing through a static arrangement of blades, the stream attains a high velocity swirl. The stream continues through a nozzle, where it is accelerated to high sub-sonic or to supersonic speeds. Due to the rapid expansion at the exit of the nozzle the desired condensates will form as a mist. The centrifugal force of the swirl moves those liquids as a film to the wall where they run off through a suitable constructive arrangement and are diverted together with some slip gas. The gas stream continues through an anti-swirling arrangement and through diffusers. Here the stream is slowed down and the kinetic energy converts back into pressure, regaining about 75-80% of the inlet pressure.

This technology is suitable for on-shore plants, particularly useful for off-shore plants due to the small footprint and reduced weight and has a great future for subsea installations.



### 2.6.2 TWISTER supersonic separator

The Twister Supersonic Separator is a combination of physical processes producing a completely revolutionary gas conditioning system. Condensation and separation at supersonic velocity is the key to achieving a significant reduction in both capital and operating costs. The simplicity and reliability of Twister technology enables de-manned, or not normally manned, operation in harsh onshore and offshore environments and is expected to prove to be a key enabler for sub-sea gas processing. In addition, the compact and low weight Twister system design enables de-bottlenecking of existing space and weight constrained platforms.

The Twister Supersonic Separator has thermodynamics similar to a turbo-expander, combining expansion, cyclonic gas/liquid separation and re-compression in a compact, tubular device. Twister achieves temperature drop by transforming pressure to kinetic energy. The centrifugation force generated by the cyclonic flow in the twister can go up to 500,000g in order to achieve supersonic flow and swelling effect. The diagram of twister supersonic separator is shown in Figure 4.

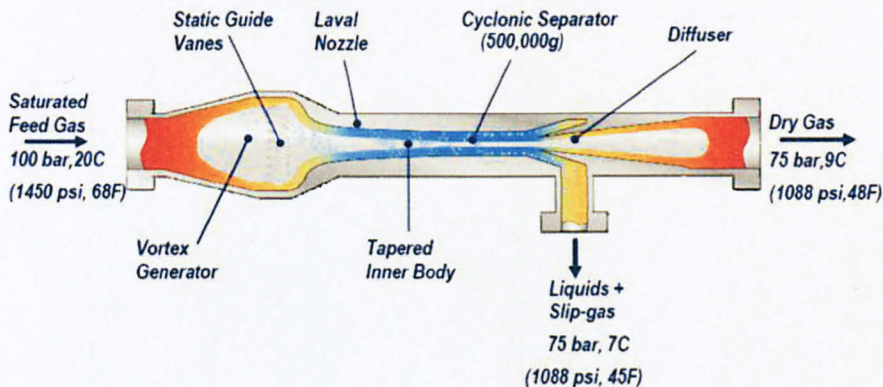


Figure 4: Twister supersonic separator

A Laval nozzle is used to expand the saturated feed gas to supersonic velocity, which results in a low temperature and pressure. This results in the formation of a mist of water

and hydrocarbon condensation droplets. The high vorticity swirl centrifuges the droplets to the wall. The liquids are split from the gas using a cyclonic separator. The separated streams are slowed down in separate diffusers, typically recovering 70 - 75% of the initial pressure. The liquid stream contains slip-gas, which will be removed in a compact liquid de-gassing vessel and recombined with the dry gas stream.

Twister BV is currently working on a joint technology development project with Petrobras in Brazil for sub-sea gas processing using Twister technology. The first commercial offshore Twister application started-up in December 2003 on Petronas/Sarawak Shell Berhad B11 facility offshore East Malaysia to dehydrate 600 MMscfd of non-associated sour gas fed to the onshore Malaysian LNG plant at Bintulu, Sarawak to control pipeline corrosion.

### CHAPTER 3: METHODOLOGY

Figure 5 depicts the methodology employed in all phases of the project. Gantt chart which illustrates project schedule can be found in APPENDIX A. FLUENT and GAMBIT software are used to perform the simulation. GAMBIT is the preprocessor for FLUENT to setup geometry and generate mesh. The geometry is then export to FLUENT where it models fluid flow and heat transfer in the geometry.

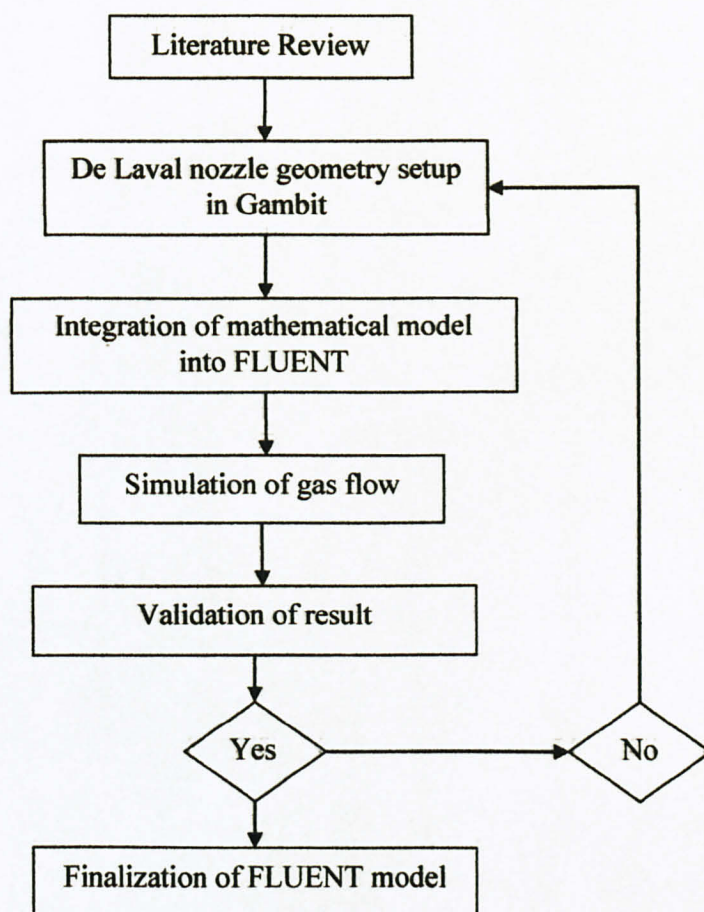


Figure 5; Project Flow Chart



## CHAPTER 4 RESULT AND DISCUSSION

### 4.1 2D Modeling and Simulation

#### 4.1.1 Gambit Drawing

Supersonic nozzle is drawn and meshed using Gambit, with finer mesh at area nearer to the convergent and divergent sections as properties changes are significant there. Figure 6 shows the drawing of the nozzle.

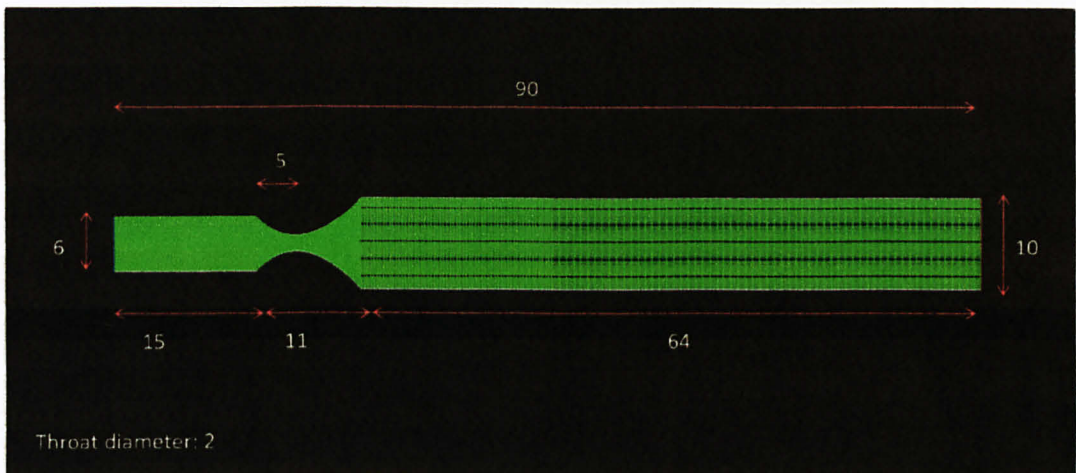


Figure 6: Gambit 2D drawing of convergent-divergent nozzle (unit in meter)

#### 4.1.2 Fluid flow simulation

The velocity of the flow is expected to increase when it passes through the converging part until it achieves the supersonic flow, 460 m/s (Mach =1) at the throat. After the throat, it will flow through divergence part and the natural gas will experience swelling effect which causes temperature and pressure drop. The water will be condensed into water droplets; hence reducing water vapor content in pipe.

The velocity profile (Figure 7) obtained from FLUENT simulation is similar with the hypotheses but does not fully agree with it, where velocity of gas increases as it approaches the convergent section. Velocity reaches maximum at the center of the throat,



where cross section area is the smallest of the system. However, the highest velocity achieved is 180 m/s, which is lower than the speed of sound in methane (460 m/s). Thus Mach number is lower than unity and the gas is in subsonic flow throughout the system. Flow rate decreases as the gas flows through the divergence part. In contrast, if supersonic flow is attained gas will keep accelerating during expansion. Besides, gas near to the wall has lower velocity due to frictional force.

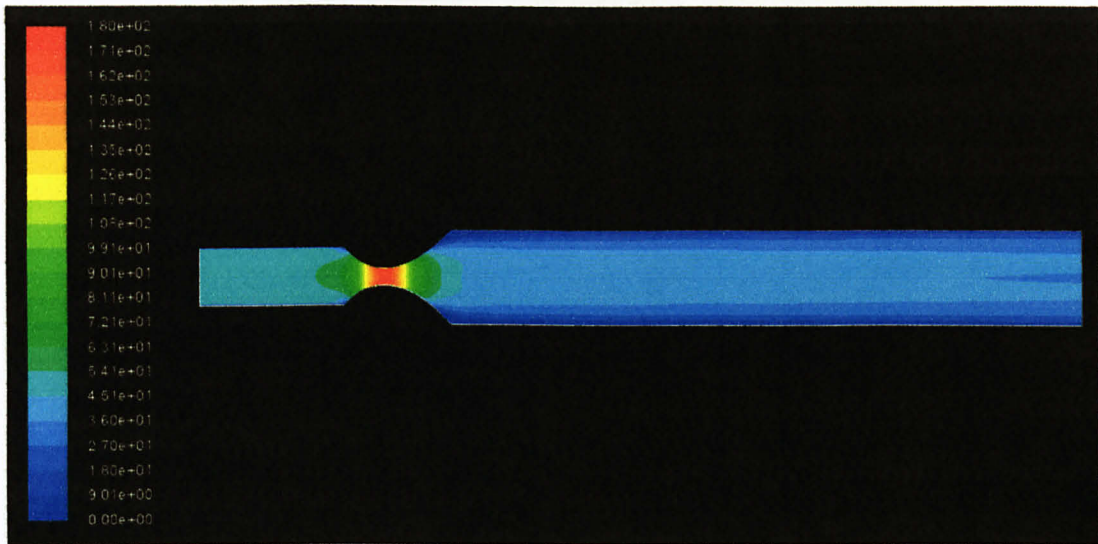


Figure 7: Velocity profile in unit m/s

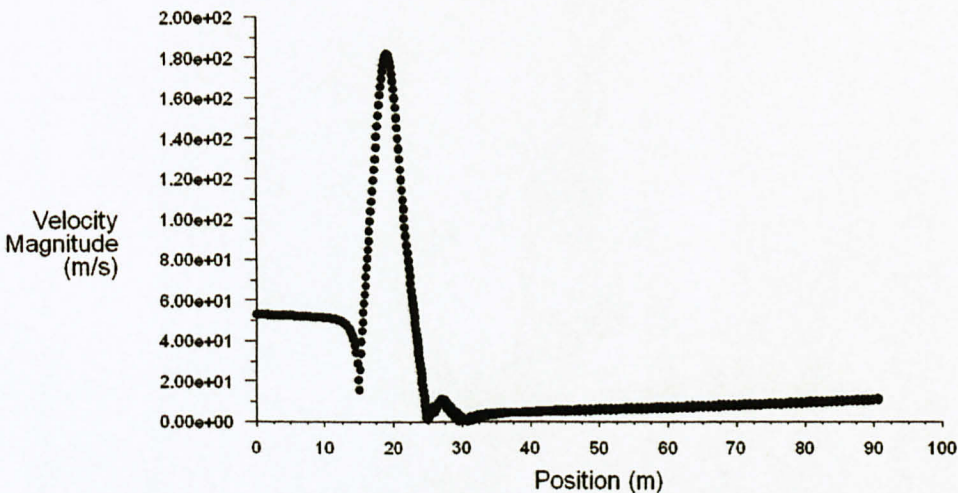


Figure 8: Velocity distribution along x-direction

Temperature drops 13K, from its initial temperature of 318K to 286K at the throat as shown in Figure 9 and Figure 10. This demonstrates Joule-Thomson effect when gas is forced through a much smaller area.

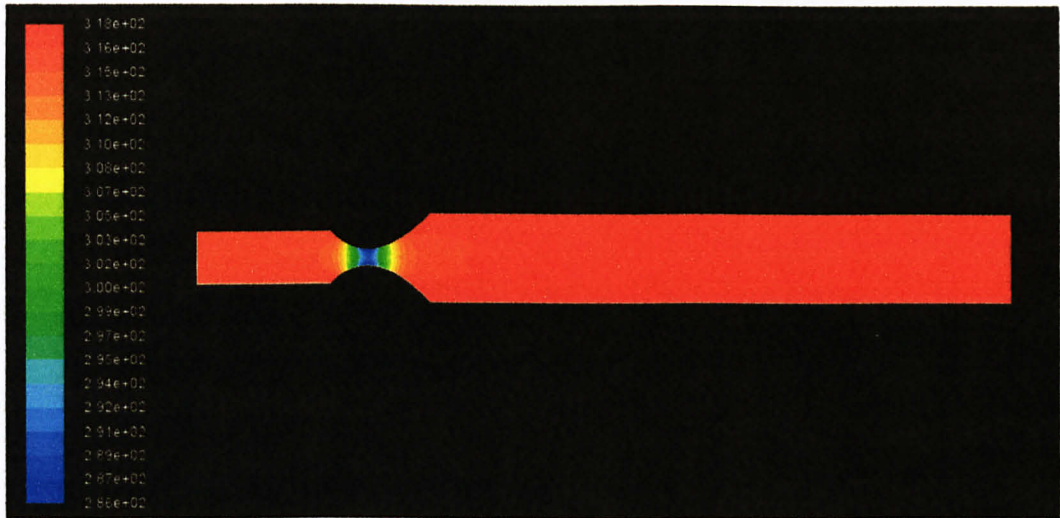


Figure 9: Temperature profile in unit Kelvin

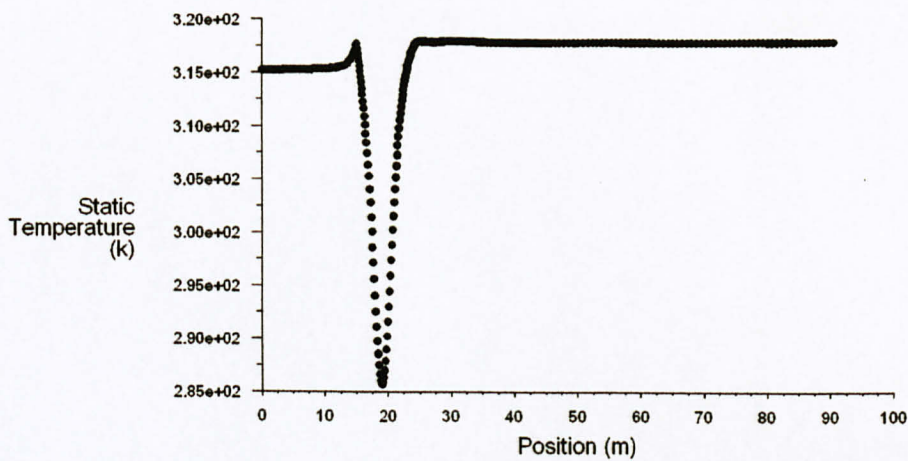


Figure 10: Temperature distribution along x-direction

Significant pressure drop is observed across the choke due to the constriction that raises velocity of the gas mixture. Pressure profile and pressure distribution along x-direction is shown in Figure 11 and Figure 12.

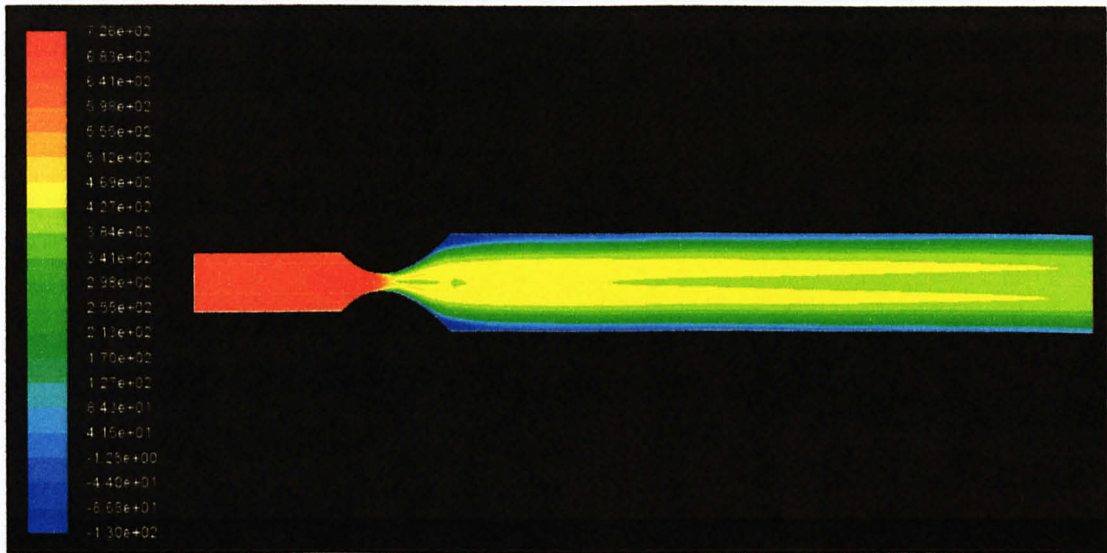


Figure 11: Pressure profile in unit Pascal

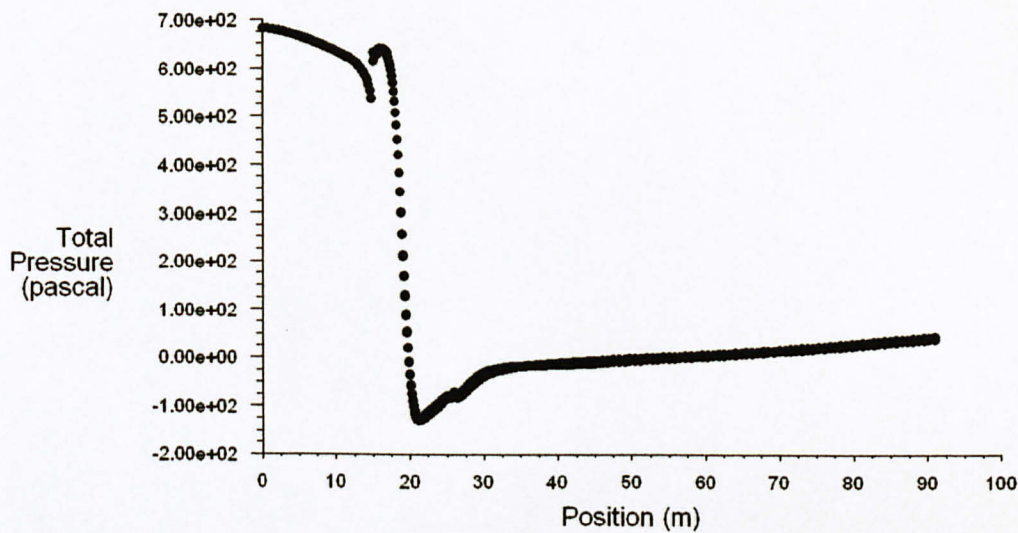


Figure 12: Pressure distribution along x-direction



A small amount of water is condensed , thus lower mass fraction of water is observed downstream the choke. The lowest water fraction, which is 0.00023, is observed at the throat. Mass fraction changes of water in the system is shown in Figure 13, while Figure 14, Figure 15 and Figure 16 shows mass fraction of methane carbon dioxide and hydrogen sulphide, respectively. Generally, concentration of all components decreases near the choke.

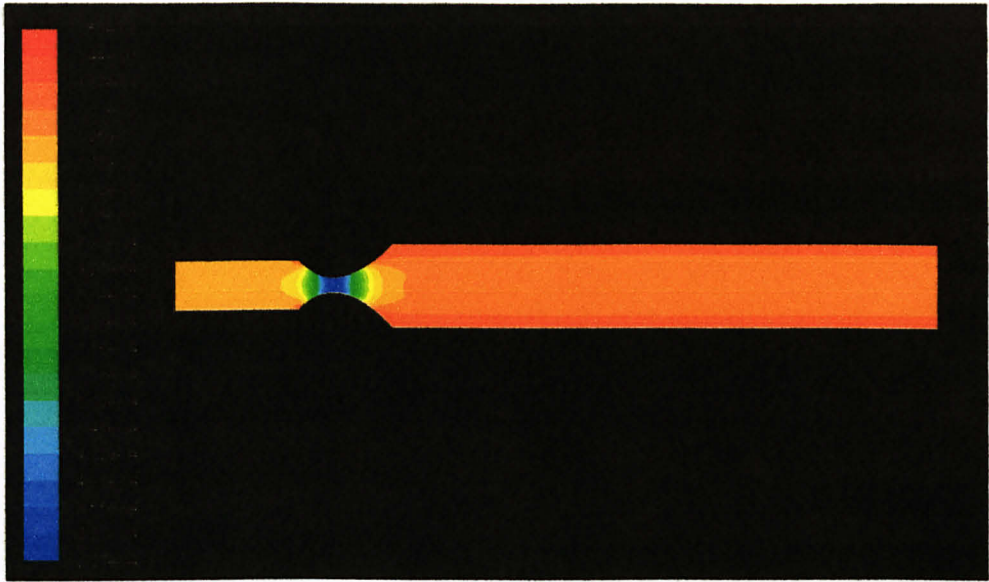


Figure 13: Mass fraction of water vapour

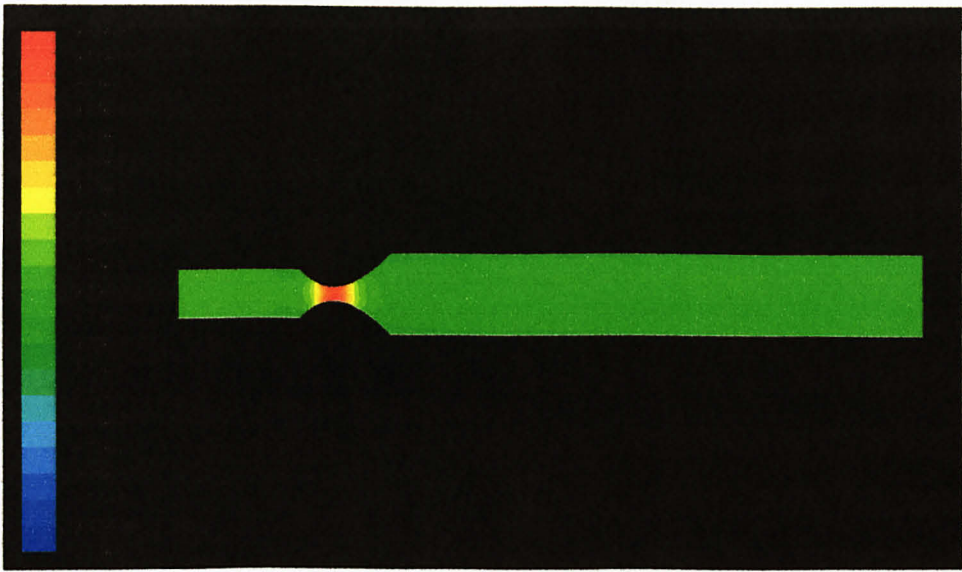


Figure 14: Mass fraction of methane

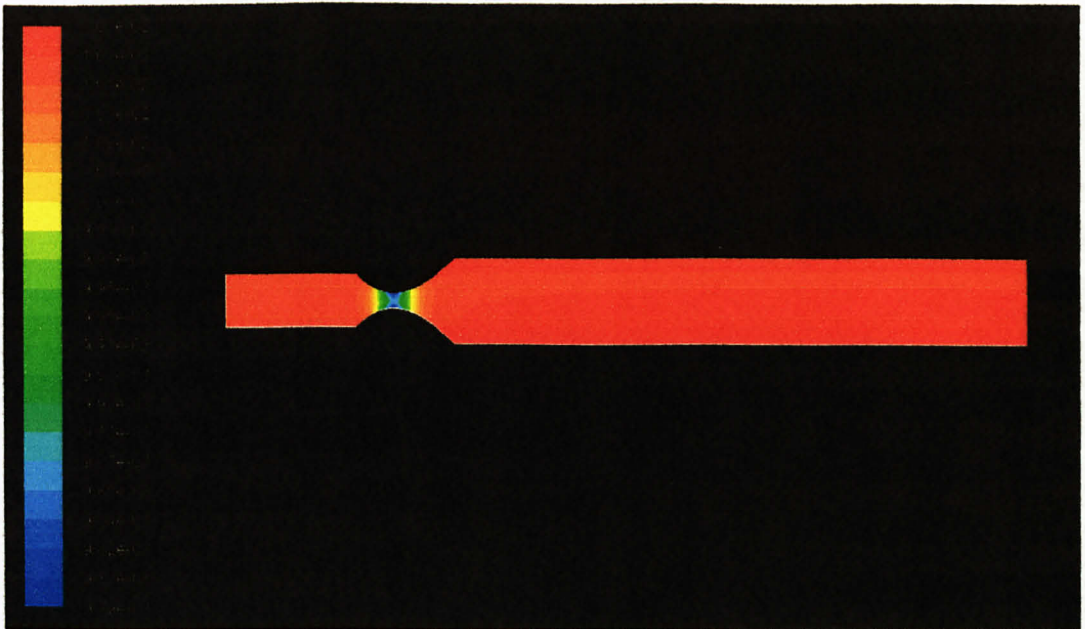


Figure 15: Mass fraction of carbon dioxide

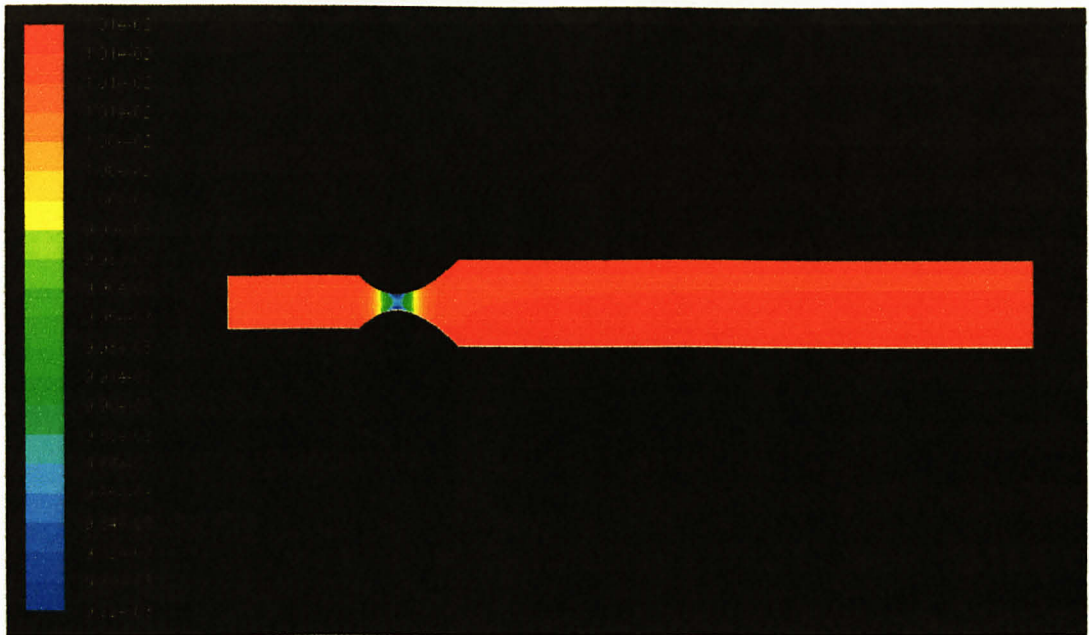


Figure 16: Mass fraction of hydrogen sulphide

#### 4.1.3 Effects of different inlet mass flow rate

The inlet mass flow rate is set at 200 kg/s for the analysis above. In this part of the report, inlet mass flow rate is varied to study its impact on velocity, temperature and efficiency in removing water. Each run is set to 10,000 iterations or achieve convergence; whichever comes first.

##### 4.1.3.1 Inlet mass flow rate at 180kg/s

Velocity and temperature profiles (Figure 17 and Figure 18) are similar with profiles at 200 kg/s. However, it has lower maximum velocity of gas, 162 m/s due to reduced mass flow rate that enters the system. As a result, temperature drop across the throat decreases, only 26 K of decrement is recorded.



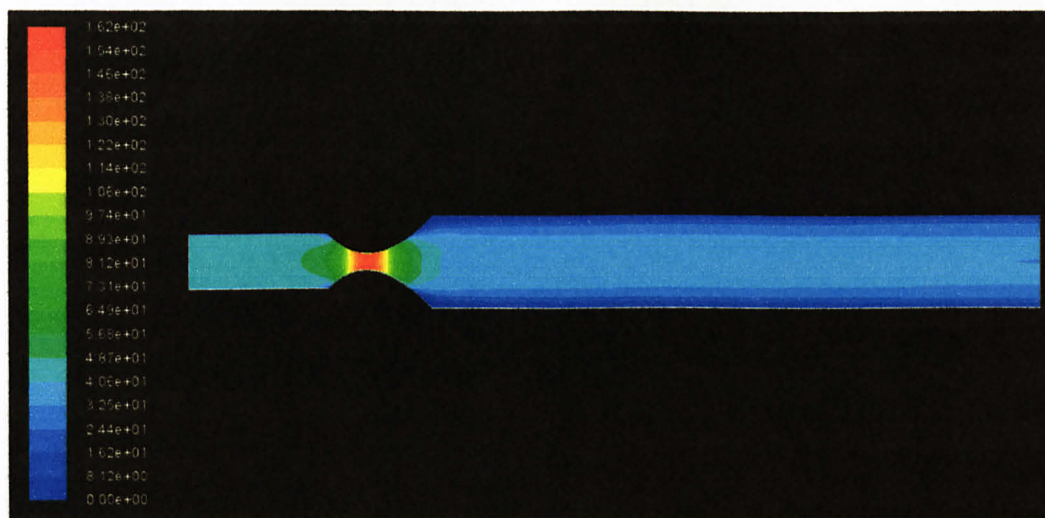


Figure 17: Velocity profile in unit m/s at inlet mass flow rate of 180kg/s

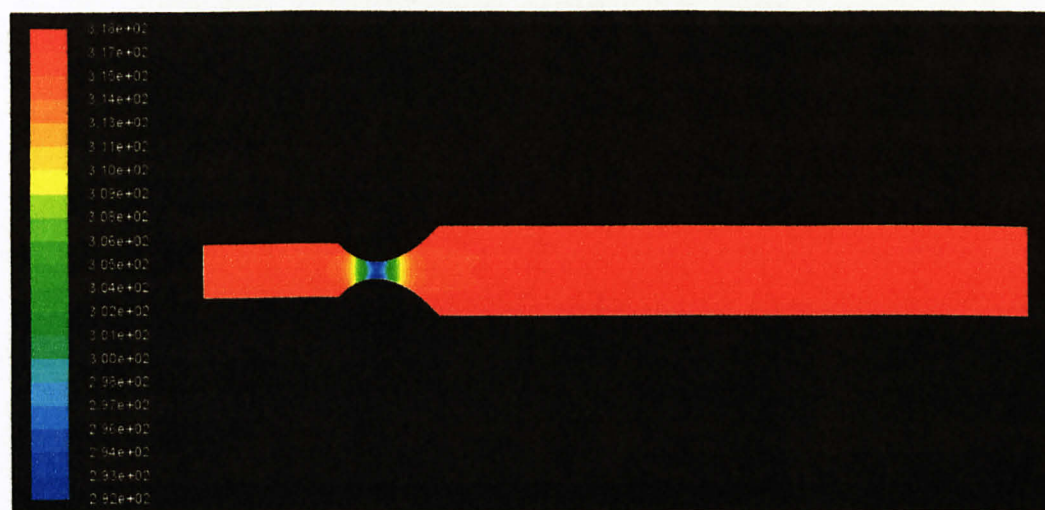
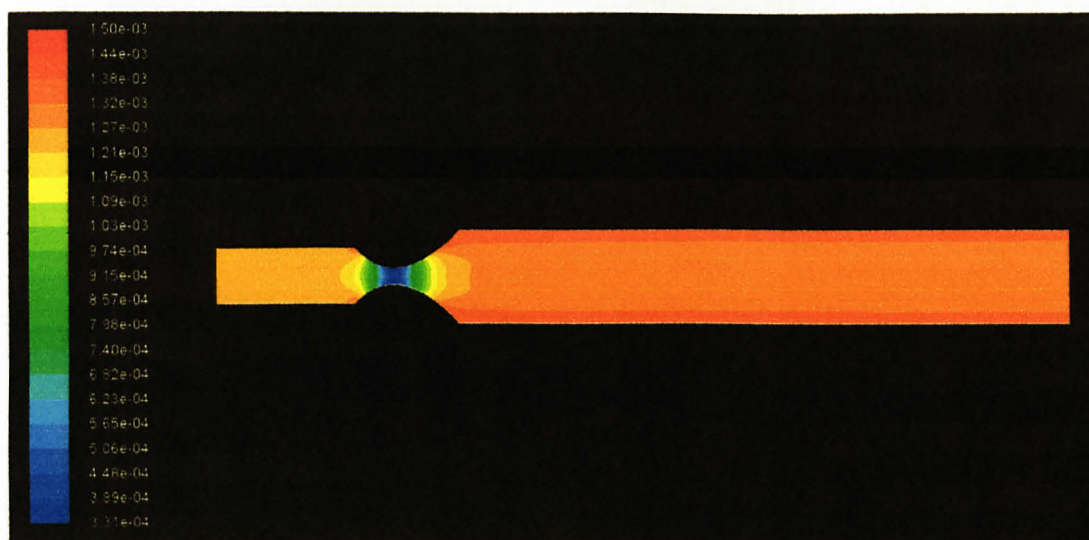


Figure 18: Temperature profile in unit Kelvin at inlet mass flow rate of 180kg/s

Mass fraction profile of water vapor is the same as profile at 200 kg/s. Mass fraction at choke is 0.00033, higher than mass fraction recorded at inlet mass flow rate of 200 kg/s.



**Figure 19: Mass fraction of water vapour at inlet mass flow rate of 180kg/s**

#### 4.1.3.2 Inlet mass flow rate at 100kg/s

When inlet mass flow rate is further lowered to 100 kg/s, velocity at throat reduces to 90.4 m/s. Cooling effect of the expansion also reduces as the temperature only drops to 310K, 8K difference from its initial temperature. Velocity and temperature profiles are shown in Figure 20 and Figure 21.

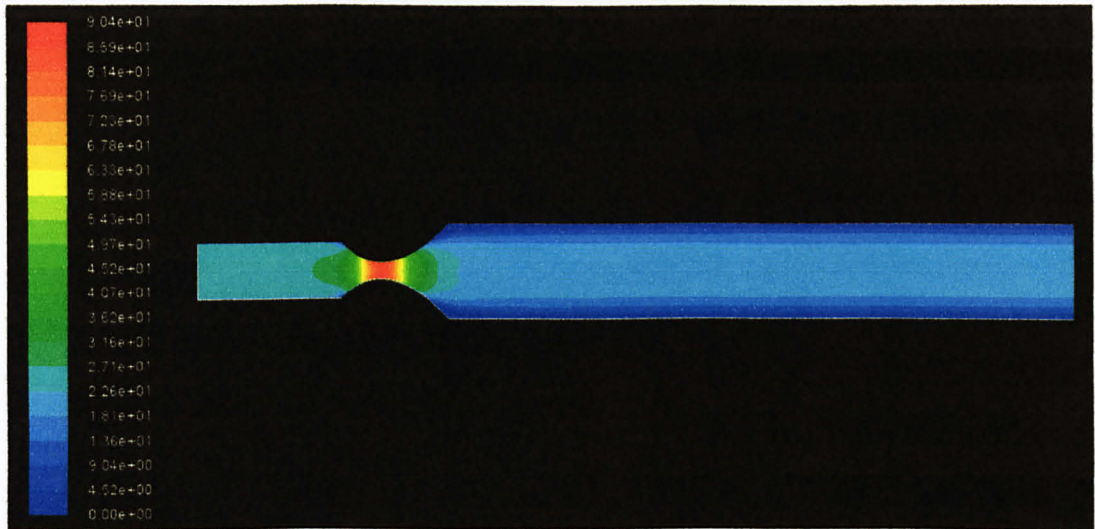


Figure 20: Velocity profile in unit m/s at inlet mass flow rate of 100kg/s

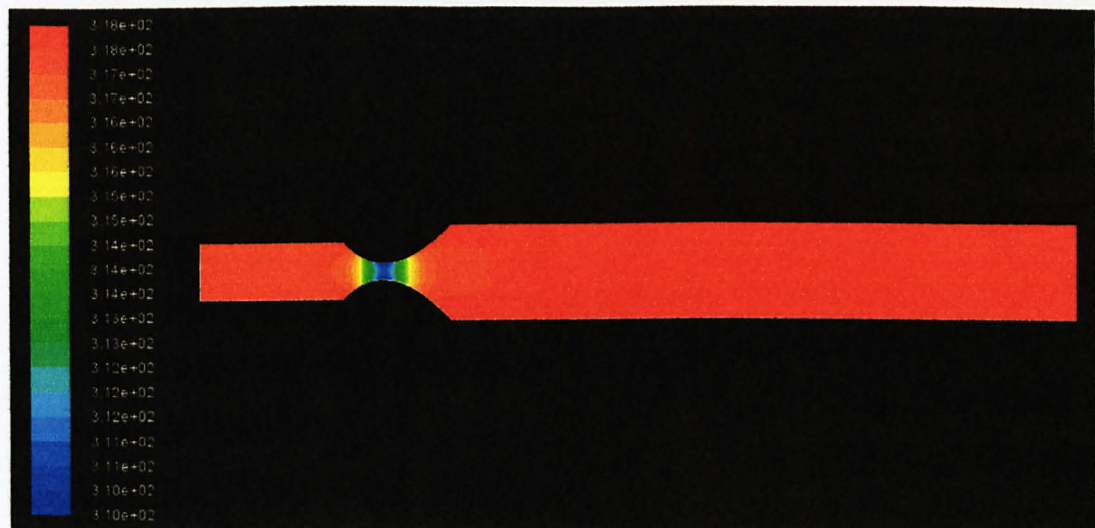


Figure 21: Temperature profile in unit Kelvin at inlet mass flow rate of 100kg/s



At inlet mass flow rate of 100 kg/s, the simulation result does not show any change in composition of the gas mixture as illustrated in Figure 22 and Figure 23. Mass fractions of all components are constant throughout the process, thus there is no phase change occur in this process.

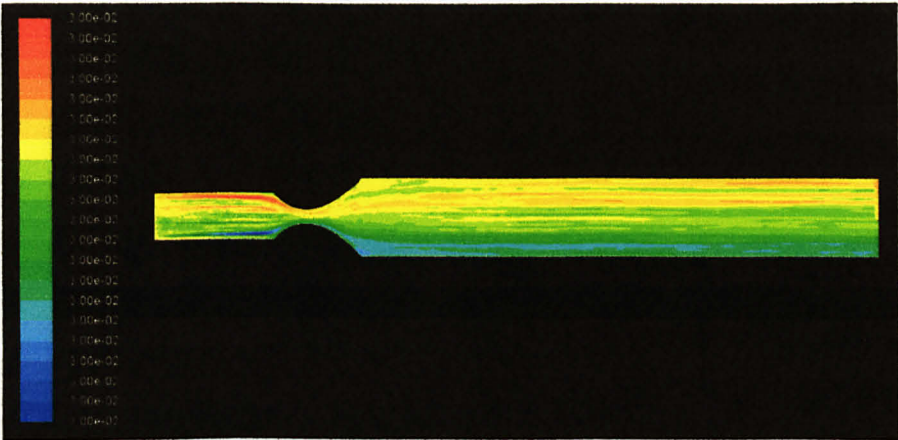


Figure 22: Mass fraction of water vapor at inlet mass flow rate of 100kg/s

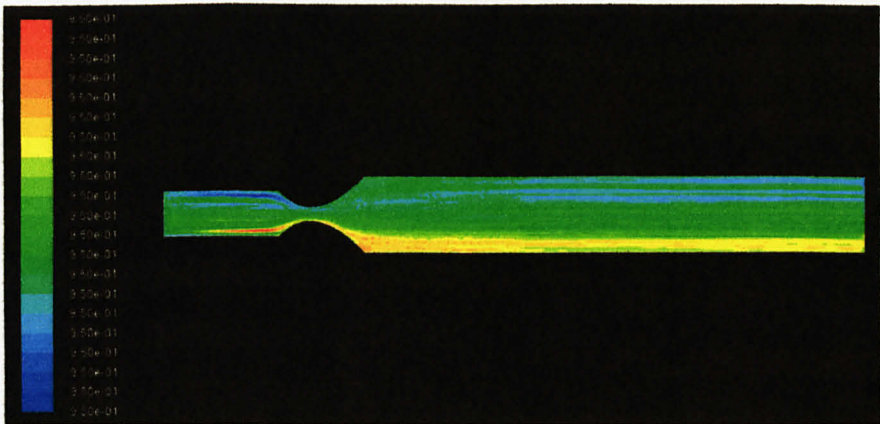


Figure 23: Mass fraction of methane at inlet mass flow rate of 100kg/s

## 4.2 3D Modeling and Simulation

### 4.2.1 Gambit Drawing

Another drawing of nozzle in pipeline is done in 3D to model more comprehensive behavior of fluid flow. Dimension of drawing is smaller (3 inch pipe) in correspondence to existing prototype of the system. In order to ensure fluid profile is fully developed at the outlet, length of pipe after choke is increased. As in 2D drawing, finer mesh is applied at area nearer to the convergent and divergent sections. Geometry and dimension of convergent-divergent nozzle is shown in Figure 24.

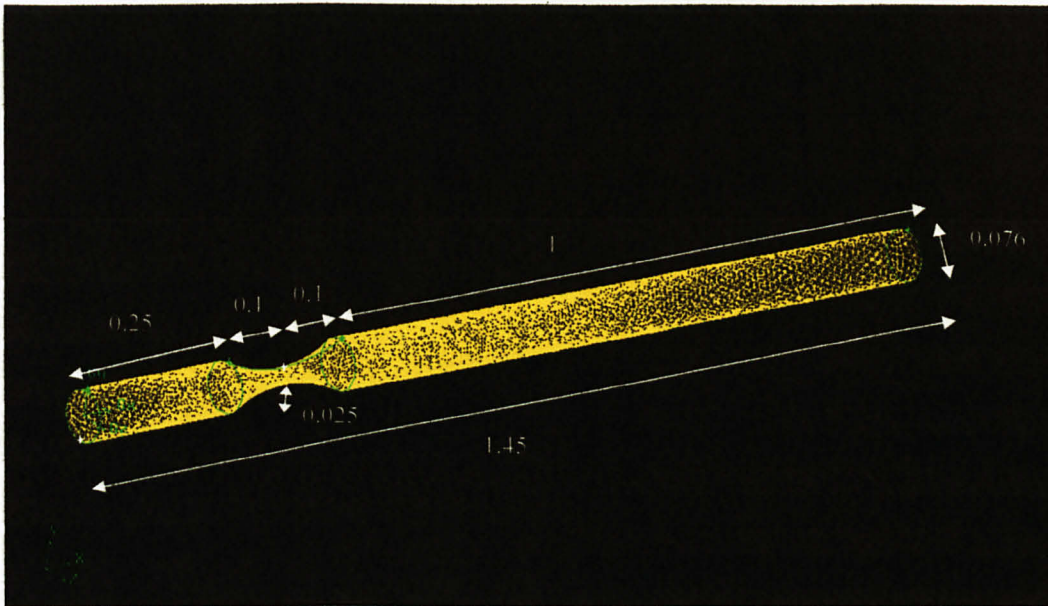


Figure 24: Gambit 3D drawing of convergent-divergent nozzle (unit in meter)

### 4.2.2 Fluid flow simulation

Natural gas flow through De Laval nozzle is simulated at varying inlet mass flow rates, with increase of 0.5kg/s from 2kg/s to 5.5kg/s. Following are the parameters specified for the simulation.

Table 1: Simulation inputs

Temperature	320 K	
Pressure	70 bar	
Species input mass fraction	Methane	0.082
	Hydrogen sulfide	0.05
	Carbon dioxide	0.12
	Water	0.01

The section follows show the simulation result of case of 4kg/s and 5kg/s. Other simulation results can be found in APPENDIX B.



#### 4.2.2.1 Inlet Mass Flow Rate 4 kg/s

As shown in Figure 25 and Figure 26 drastic pressure drop is witnessed at the convergent section of the nozzle due to conservation energy as fluid velocity increases through the constriction resulting in gain in kinetic energy. The lowest pressure recorded is 37.72bar at the throat. About 90% pressure recovery is observed after the throat.

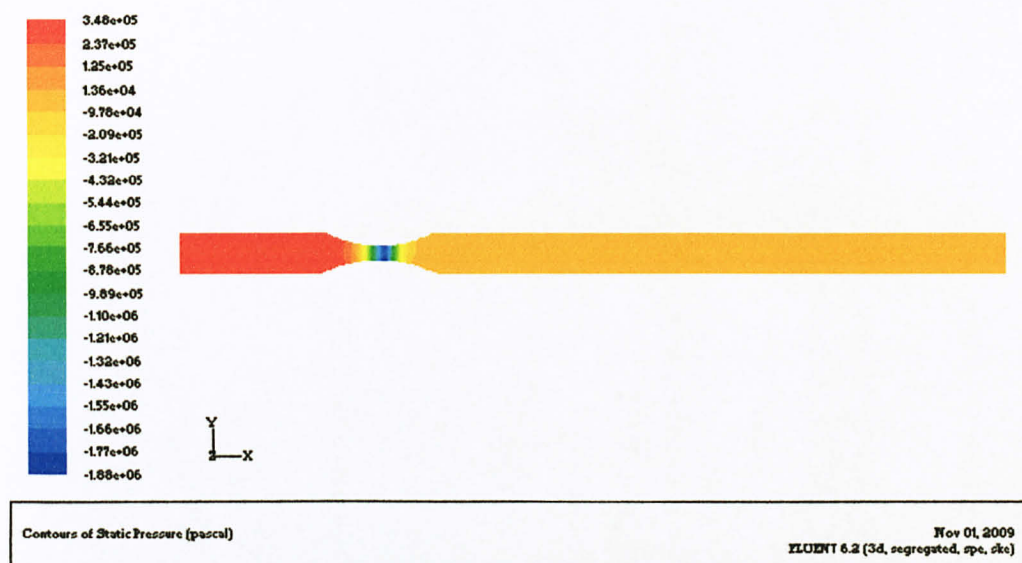


Figure 25: Static pressure profile at inlet mass flow rate of 4kg/s

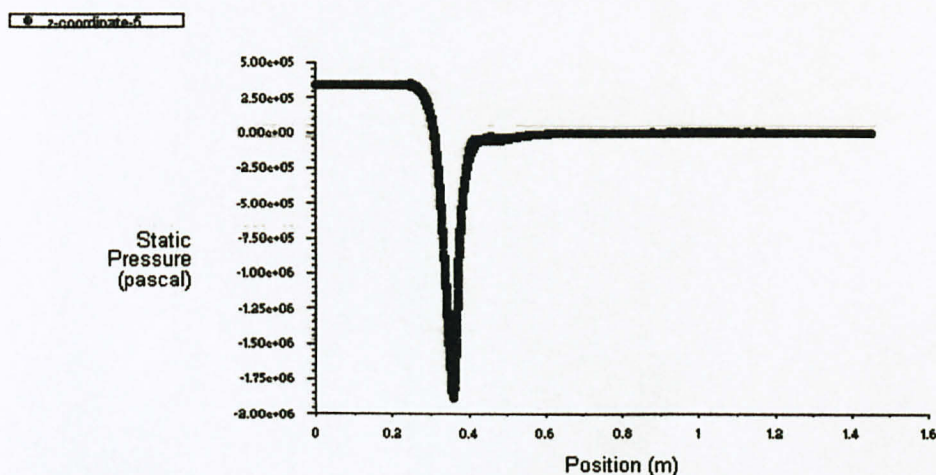


Figure 26: Static pressure distribution along x-axis at inlet mass flow rate of 4kg/s

Velocity of fluid increased as it is forced to converge to go through the smaller cross sectional area. Figure 29 shows a sharp increased in velocity at 0.35m x-direction, which is the throat position where fluid achieved its highest velocity of 432m/s. Increase in flow area at divergent section reduces the velocity of fluid flow.

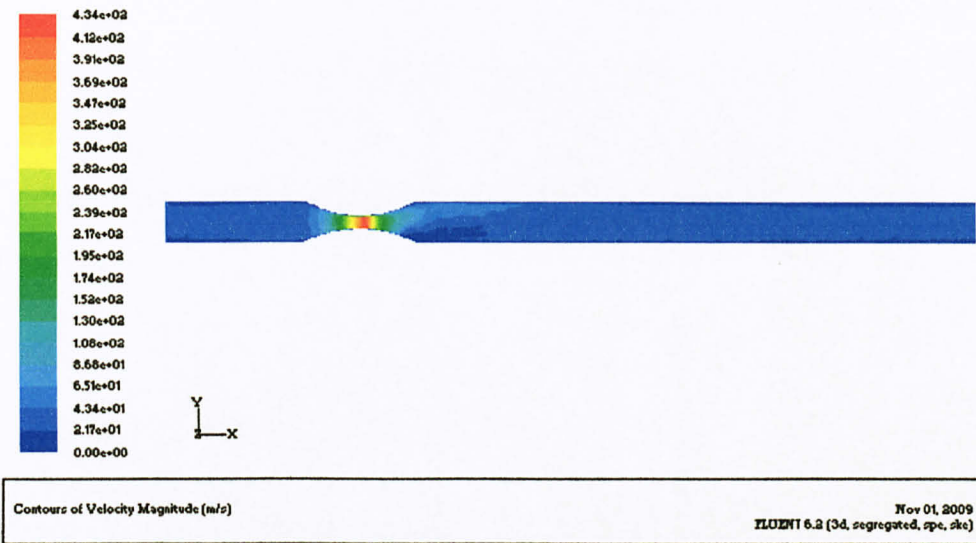


Figure 27: Velocity profile at inlet mass flow rate of 4kg/s

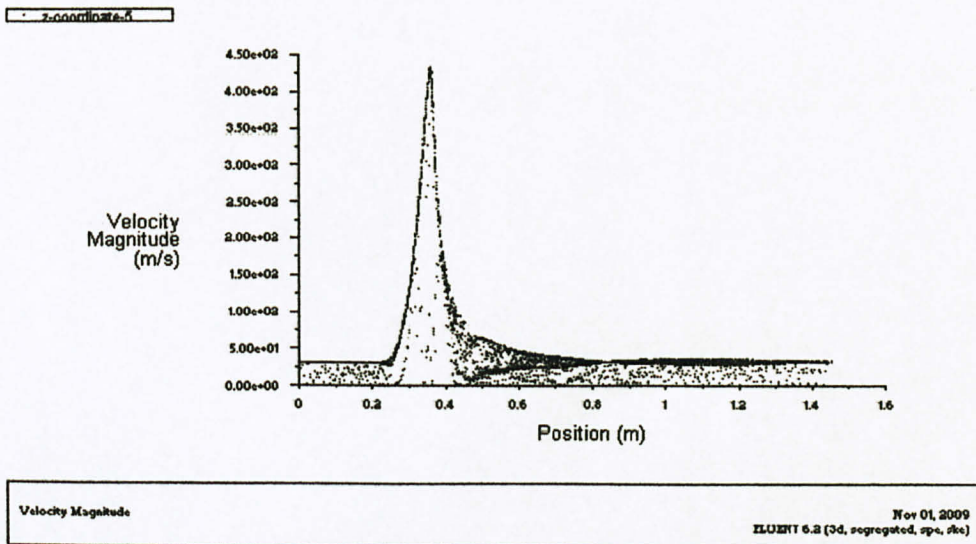


Figure 28: Velocity distribution along x-axis at inlet mass flow rate of 4kg/s

Natural gas flow approaches local speed of sound near the choke, where its Mach number is equal to 0.943.

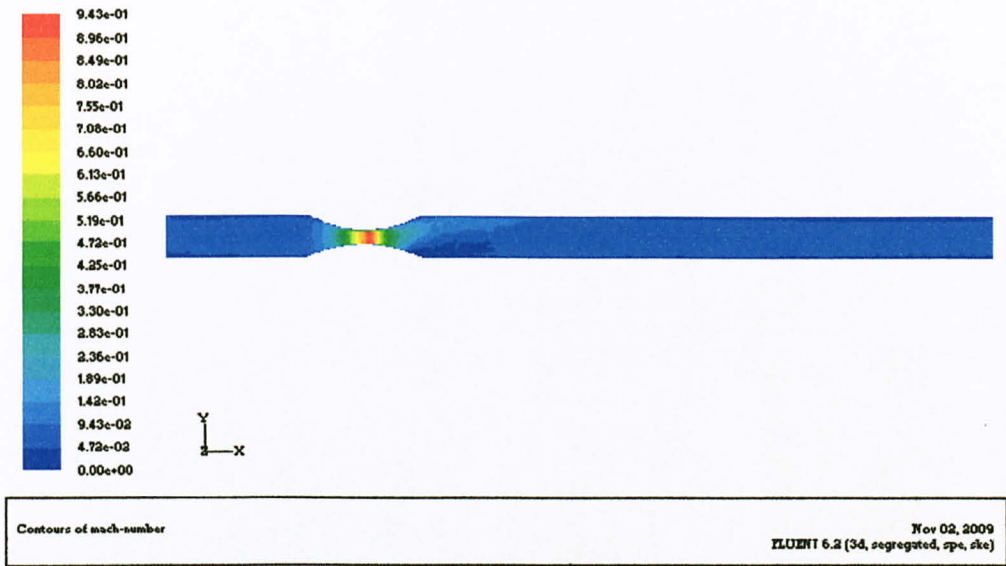


Figure 29: Mach number at inlet mass flow rate of 4kg/s

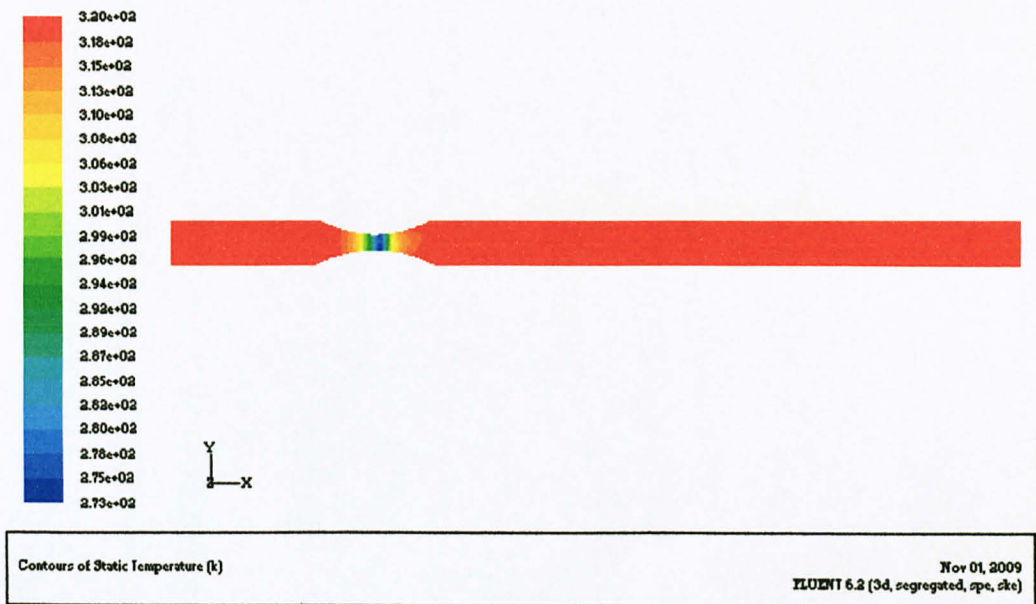
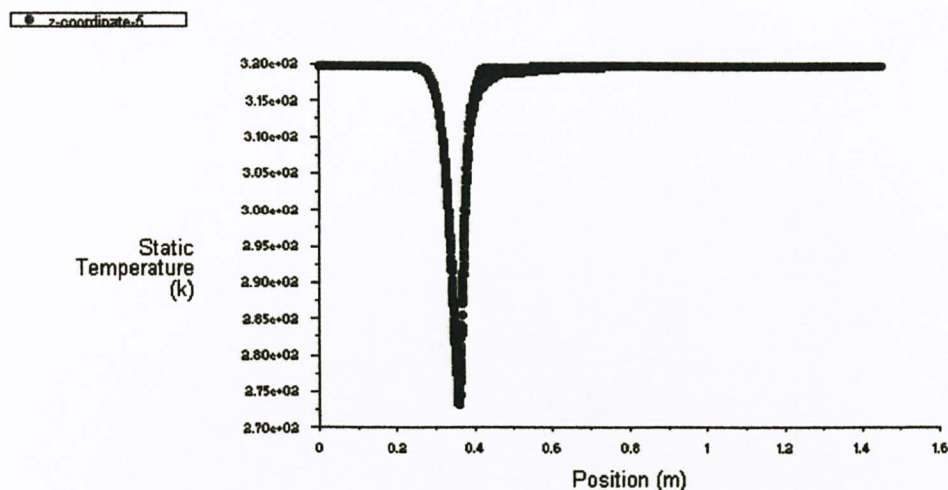


Figure 30: Temperature profile at inlet mass flow rate of 4kg/s



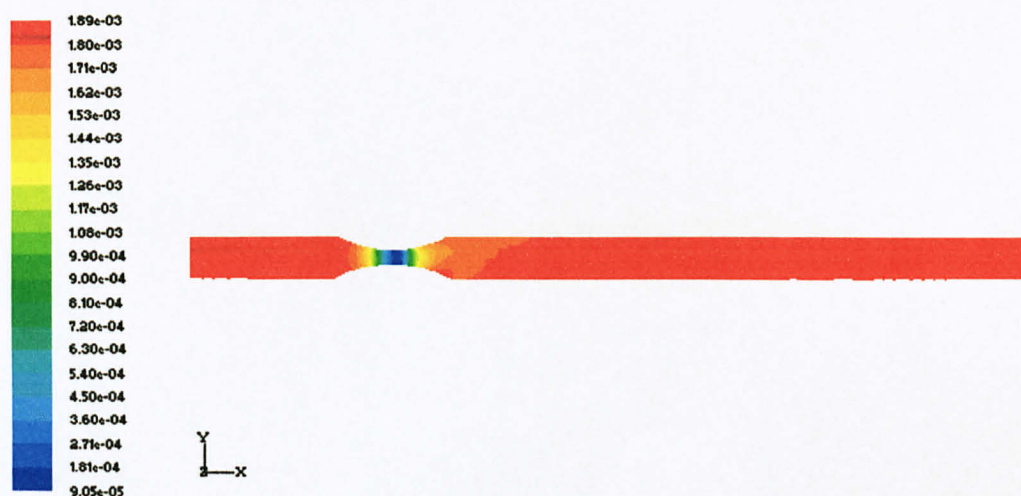


Static Temperature

Nov 01, 2009  
FLUENT 6.2 (3d, segregated, smp, ssc)

Figure 31: Temperature distribution along x-axis at inlet mass flow rate of 4kg/s

When natural gas enters the nozzle water vapor is cooled and condensed as temperature decreases significantly. Molar concentration profile of water vapour is depicted in Figure 32. However, concentration of water vapour increases as temperature raises downstream the throat area.

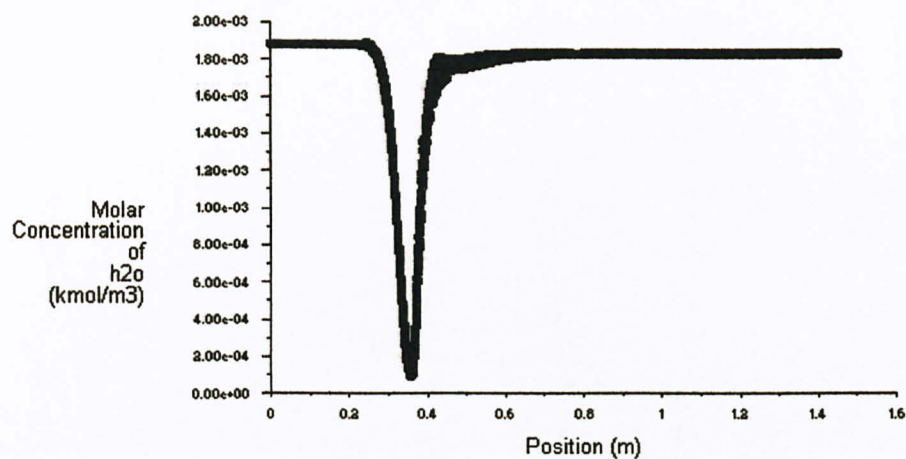


Contours of Molar Concentration of H<sub>2</sub>O (kmol/m<sup>3</sup>)

Nov 01, 2009  
FLUENT 6.2 (3d, segregated, smp, ssc)

Figure 32: Molar concentration profile of water vapor at inlet mass flow rate of 4kg/s

2-coordinate-6



Molar Concentration of h2o

Nov 01, 2009  
FLOENT 6.2 (3d, segregated, spe, ske)

Figure 33: Molar concentration distribution of water vapor along x-axis at inlet mass flow rate of 4kg/s

#### 4.2.2.2 Inlet Mass Flow Rate 5 kg/s

As compared to the case of 4kg/s inlet mass flow rate, pressure drop is higher qualitatively in this case as shown in Figure 34.

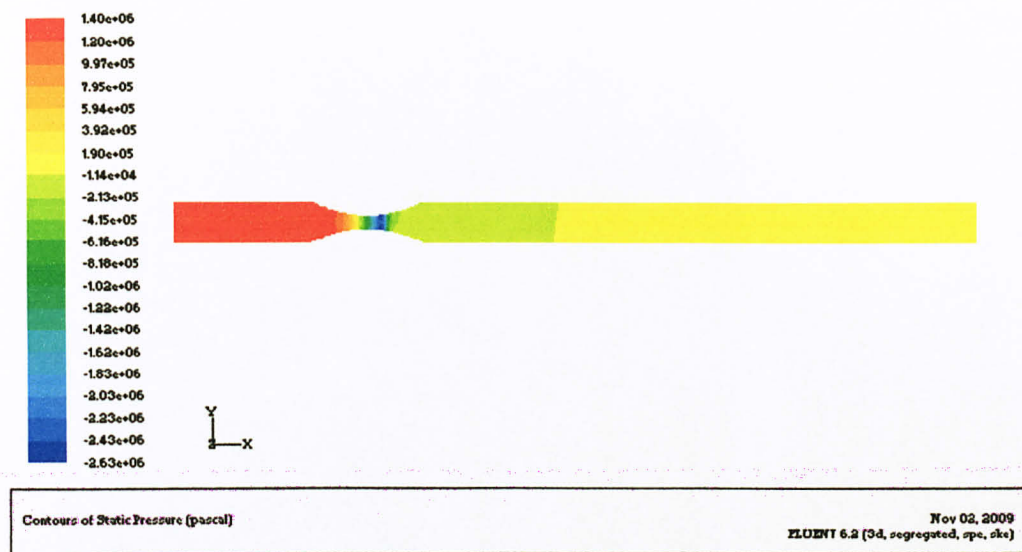


Figure 34: Static pressure profile at inlet mass flow rate of 5kg/s

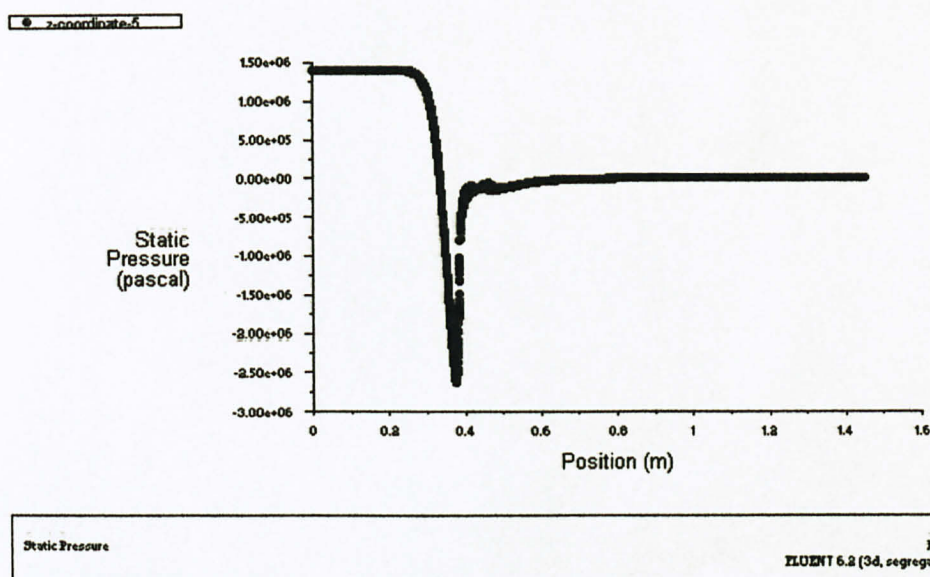


Figure 35: Pressure distribution along x-axis at inlet mass flow rate of 5kg/s



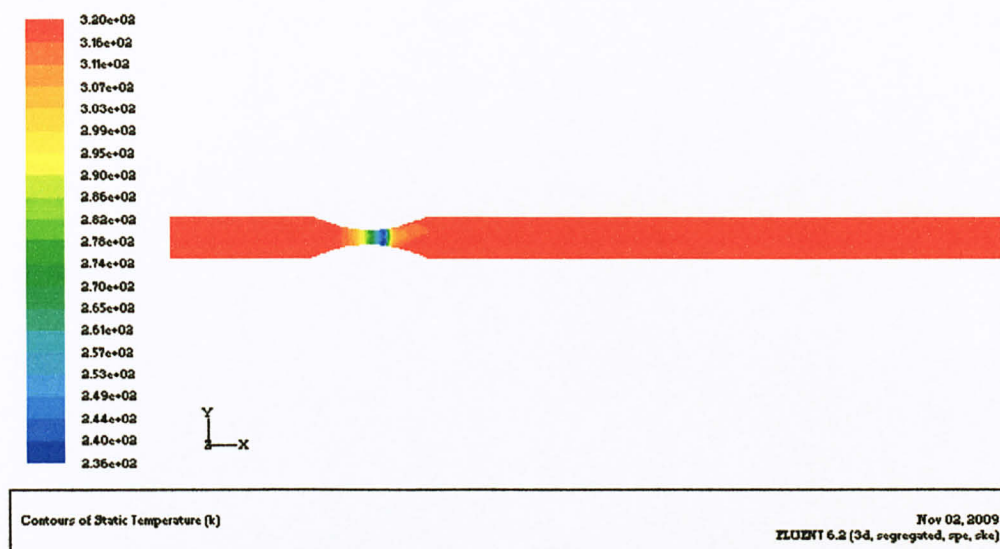


Figure 36: Temperature profile at inlet mass flow rate of 5kg/s

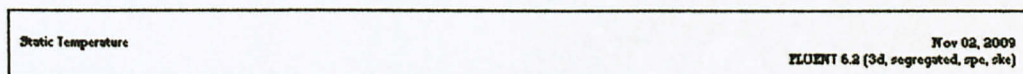
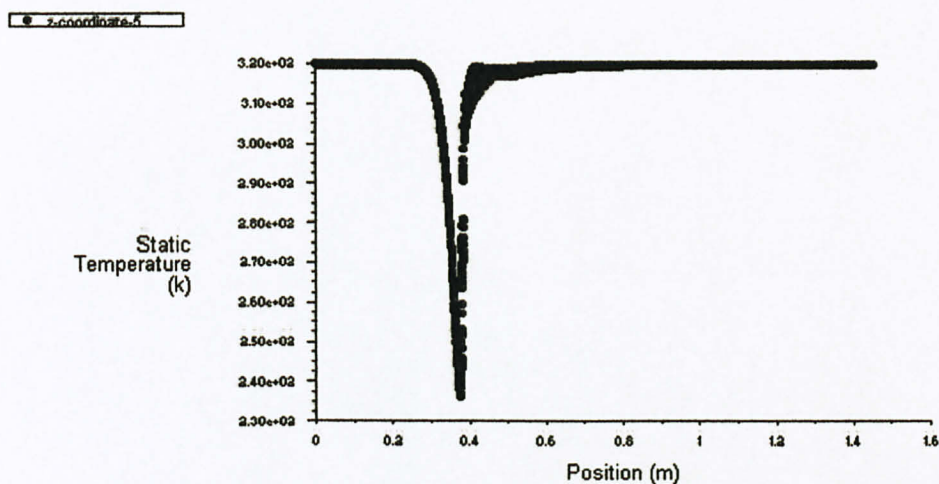


Figure 37: Temperature distribution along x-axis at inlet mass flow rate of 5kg/s

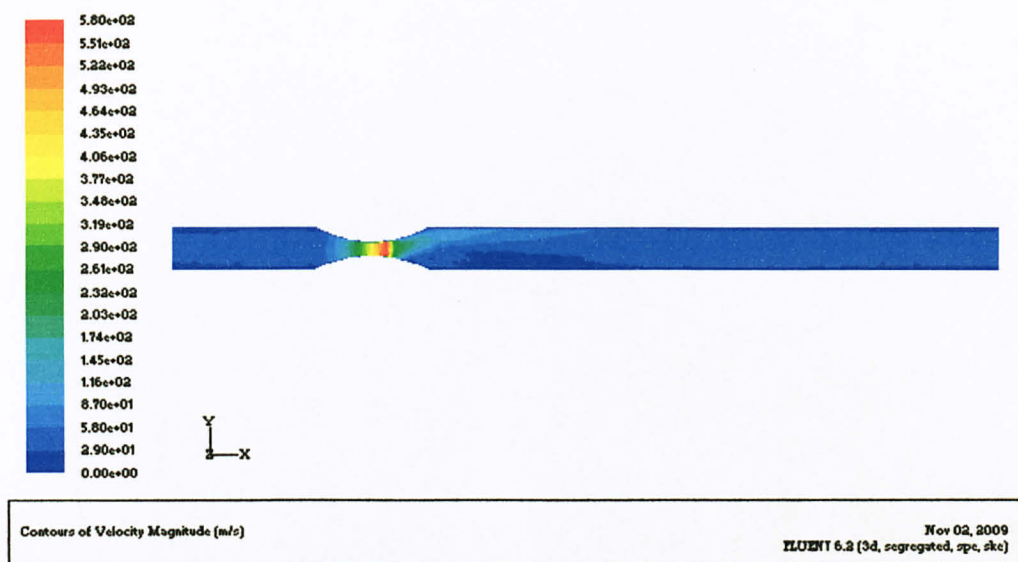


Figure 38: Velocity profile at inlet mass flow rate of 5kg/s

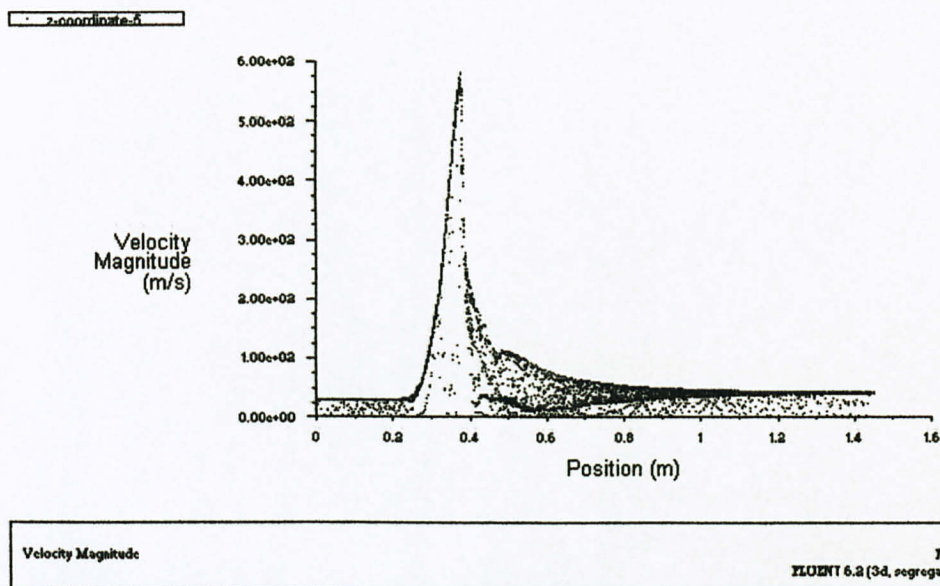


Figure 39: Velocity distribution along x-axis at inlet mass flow rate of 5kg/s

Mach number monotonically increases from inlet of nozzle to  $M=1$  at the throat, where sonic flow is achieved. The gas is further expanded to supersonic flow at the divergent part where a sound wave will not propagate backwards through the gas as viewed in the frame of reference of the nozzle. Maximum Mach number obtained is 1.26.

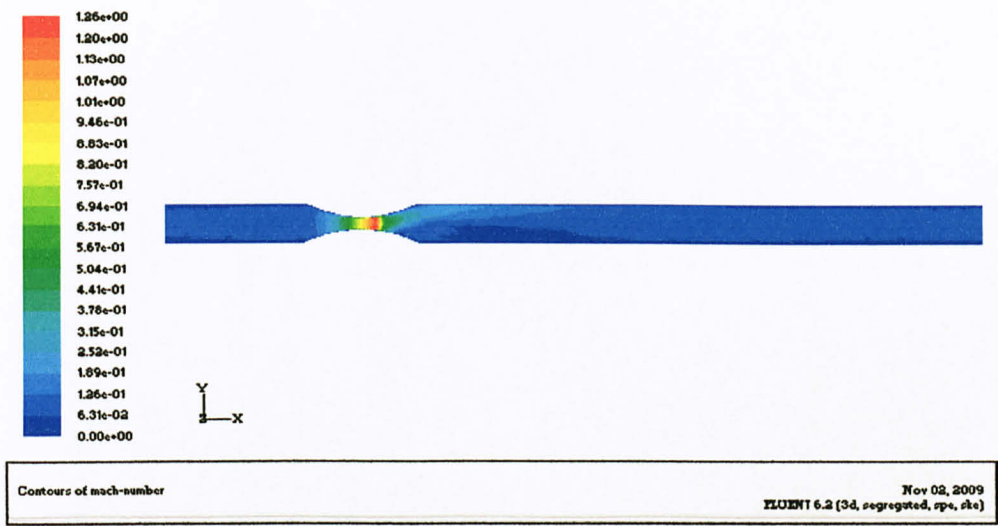


Figure 40: Mach number at inlet mass flow rate of 5kg/s

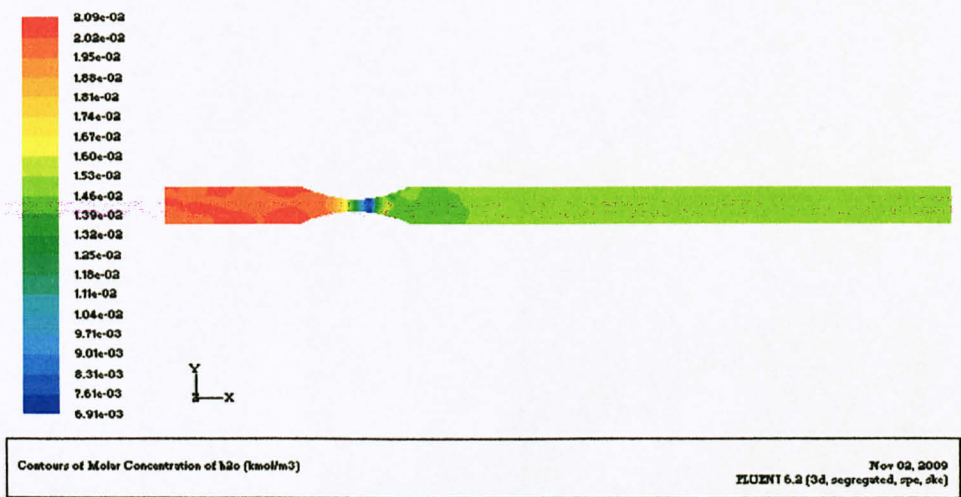
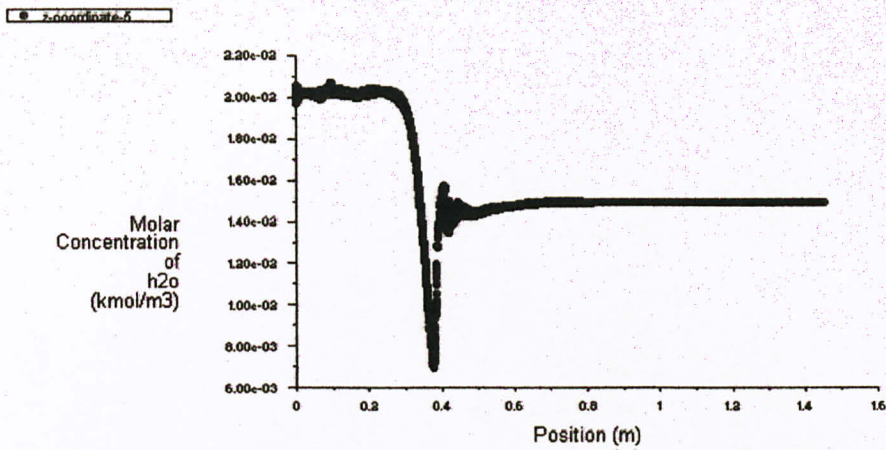


Figure 41: Molar concentration profile of water vapor at inlet mass flow rate of 5kg/s





Molar Concentration of h2o

Nov 02, 2009  
FLUENT 6.2 (3d, segregated, spe, cke)

Figure 42: Molar concentration of water vapor along x-axis at inlet mass flow rate of  $5 \text{ kg/s}$

Reduced outlet molar concentration of water vapour is can be clearly seen in this case, where water liquid does not fully vaporise after the throttling effect. Molar concentration of water vapour reduces from the initial  $0.02 \text{ kmol/m}^3$  to  $0.0015 \text{ kmol/m}^3$  at exit.

4.2.3 Summary of Simulation

Velocity is a crucial factor in reaching the desired temperature and pressure drop of gas flow through De Laval nozzle. Figure 43 illustrates the relationship of velocity with pressure at choke and temperature drop. It is found that temperature drop increases with increasing velocity while pressure at choke is lower at higher velocity. It is desirable to have large temperature drop to cool the water vapour and high pressure at choke which signifies less pressure loss in the system. Thus an optimum velocity needs to be determined to acquire sufficient temperature drop at least differential pressure.

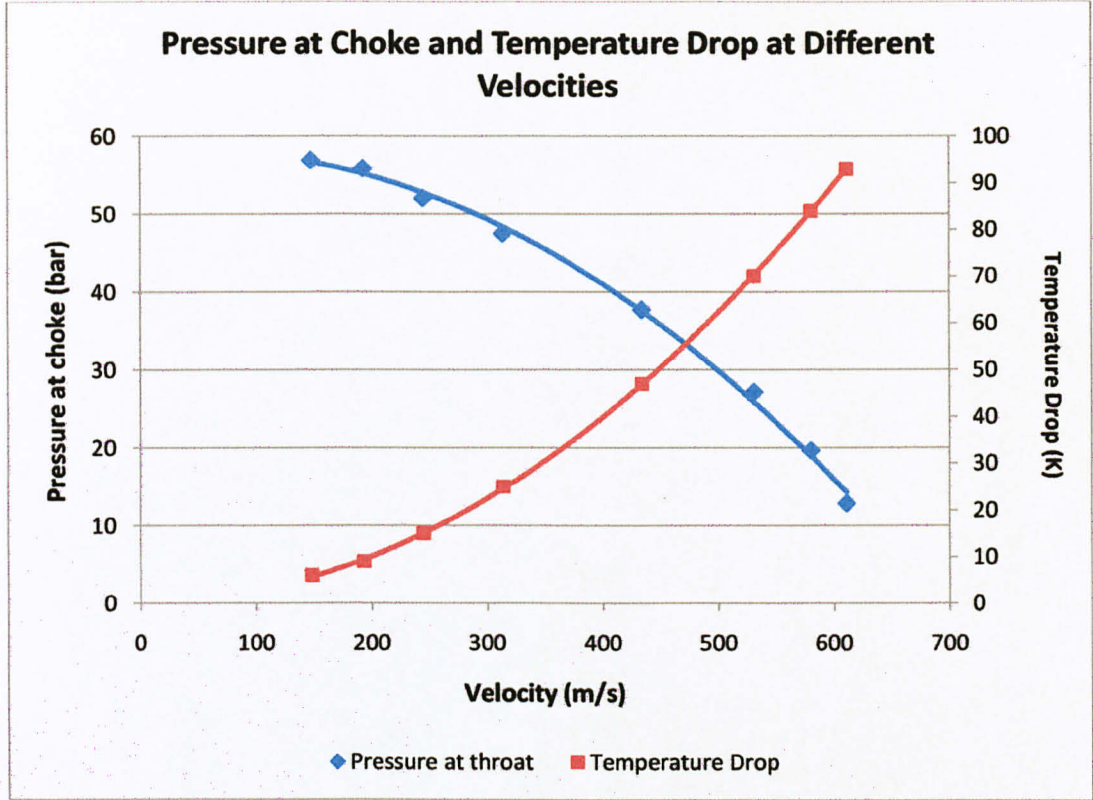


Figure 43: Pressure at choke and temperature at different velocities

Details of pressure drop, pressure at throat, temperature drop and amount of water removed are shown in Table 2.

Table 2: Pressure drop, pressure at throat, temperature drop and water removed

Mass flow inlet (kg/s)	Pressure drop (bar)	Pressure at throat (bar)	Temperature drop (K)	Water removed (kg/m <sup>3</sup> )
2	3.05	56.95	6	4.7
2.5	4.09	55.92	9	6.8
3	7.92	52.08	15	11
3.5	12.47	47.53	25	19.5
4	22.28	37.72	47	47.68
4.5	32.81	27.19	70	104.31
5	40.30	19.70	84	508.97
5.5	47.10	12.90	93	710.476

Figure 44 shows effect of inlet mass flow rate on amount of water removed. Looking at the figure, it is found that the amount of water removed increases with increasing inlet mass flow rate. Highest water removal is obtained at 5.5kg/s flow rate, which records 710.48kg/m<sup>3</sup>.s.



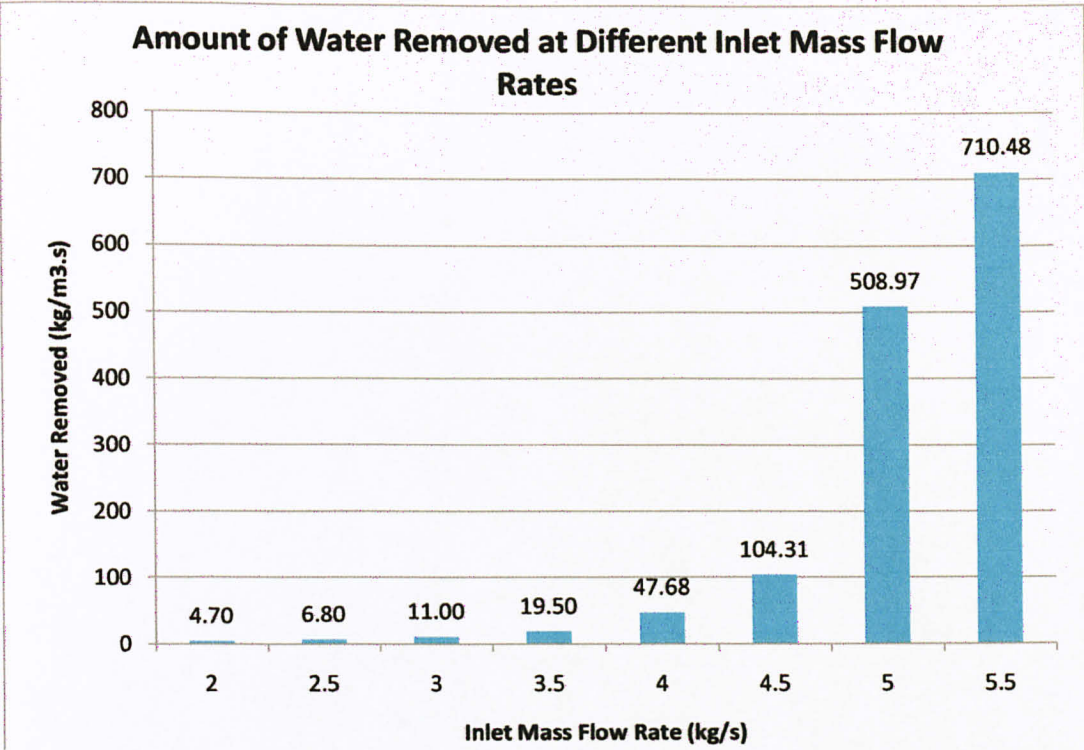


Figure 44: Water removed at different inlet mass flow rates

While it is desirable to remove larger amount of water by increasing the cooling effect, the outlet water vapour fraction shall also be checked. For example, in order to meet pipeline specification, mass fraction of water shall not exceed certain value. If fraction of water is an important criterion one has to check also the outlet fraction. There shall be an optimum design whereby it can removed large amount of water while also meeting the specification.

Higher cooling effect is capable of condensing more materials than that of lower inlet mass flow rate with lower cooling effect. Higher cooling effect could also condense out other components, particularly the valuable CH<sub>4</sub>. As a consequence, rate of removal of methane (as well as H<sub>2</sub>S and CO<sub>2</sub>) is higher resulting in increased outlet water vapour content instead of lowering it. This means higher velocity may not necessary be good for separation. Figure 45 and Figure 46 shows the outlet average mass percentage for water

vapor and outlet average mass fraction for other components, namely methane, carbon dioxide and hydrogen sulfide, accordingly.

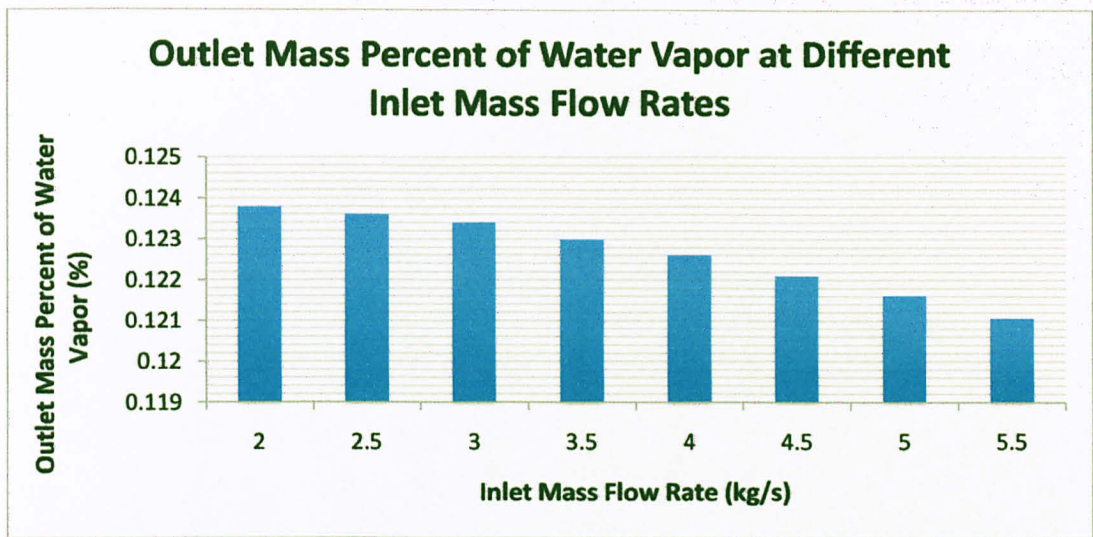


Figure 45: Outlet mass percent of water vapour at different inlet mass flow rates

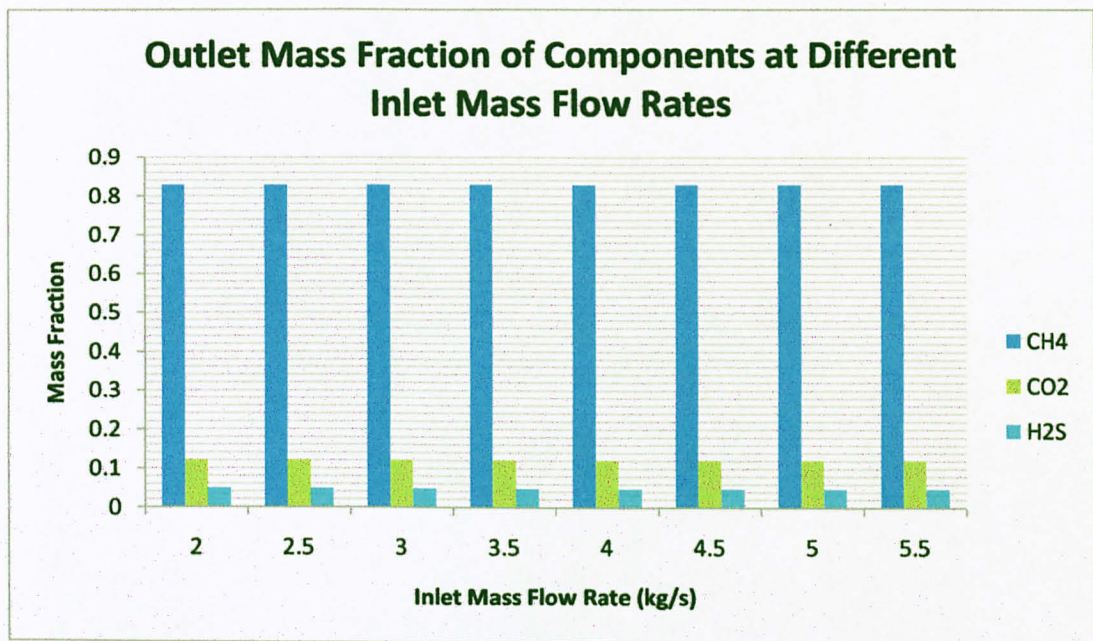


Figure 46: Outlet mass fractions at different inlet mass flow rates



From Figure 45, it is found that outlet mass percent of water decreases consistently as inlet mass flow rate is increased. On the other hand, there is no change of mass fraction of other components observed at the outlet following the cooling effect as shown in Figure 46. Hence, higher inlet mass flow rate is favoured. In addition to rate of water removed and outlet mass percent of water, other factors, such as limitation of the pipe and pumping requirement need to be taken into consideration.

**4.3 Validation of Simulation Result**

Simulation data are validated by comparing them with experimental data obtained from literature (Oil & Gas Journal, May 2005). As shown in Figure 47, simulation result is close to experimental data, showing difference of approximately  $\pm 5$  K. Therefore, the simulation model is considered valid. The values are tabulated in APPENDIX C.

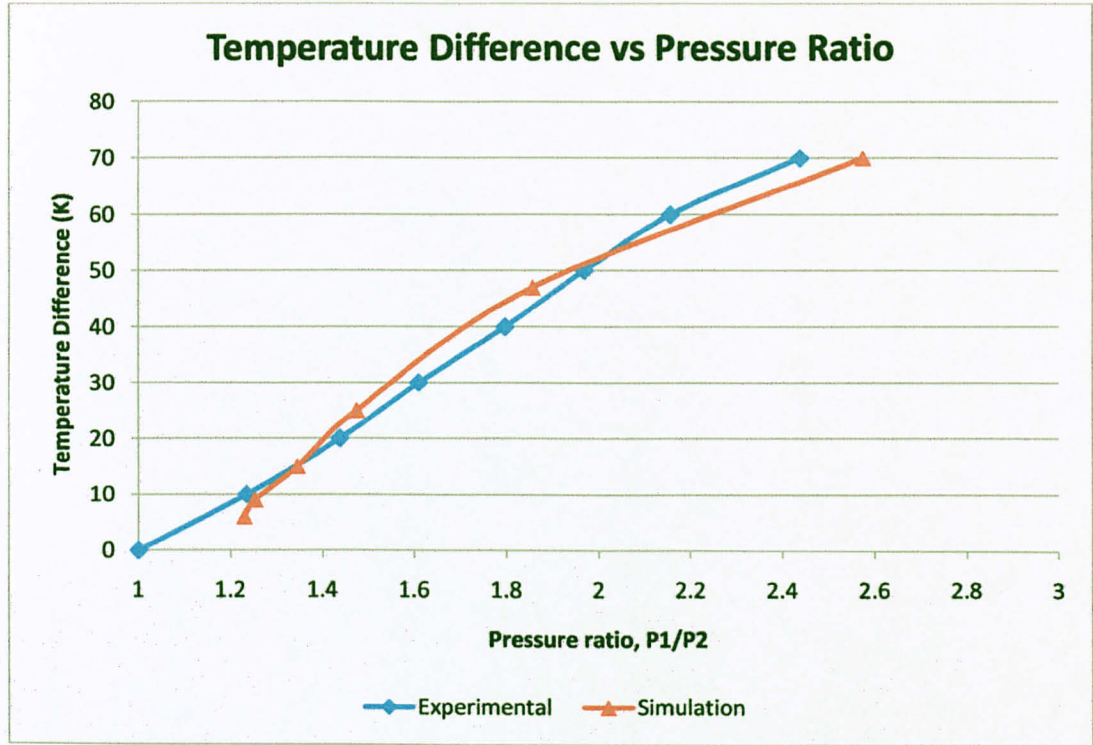


Figure 47: Comparison of simulation data and experimental data



## CHAPTER 5 CONCLUSION AND RECOMMENDATIONS

### 5.1 Conclusion

Velocity increases while temperature and pressure drop across choke due to sudden expansion is modeled using Fluent and Gambit software. Simulation result shows velocity increases as it approaches the convergent section of the nozzle and sonic flow (Mach number=1) is achieved at throat when inlet mass flow rate is sufficient. The diverging part further increases velocity of gas to supersonic velocities. Sudden expansion also decreases the pressure and temperature of the gas, which enables the system to condense water vapor, thus reducing the water vapor content in natural gas. Besides, higher inlet mass flow rate causes higher velocity at throttle, which leads to greater temperature drop and more water vapour condensed that can be removed from natural gas. Simulation result is validated with experimental data from literature.

## 5.2 Recommendations

Recommendations for future work are listed below:

1. Blades should be included in the system to create swirling effect which forces water liquid condensed to the wall and then water near the wall should be removed.
2. Generate two phase (vapour and liquid) simulation to see how much vapour is condensed to liquid and how much liquid vapourizes to gas, and how this equilibrium affects the outflow fraction. In this way, absolute amount of loss of each component can be obtained.
3. Different design of De Laval nozzle could be tested for its cooling effect and water removal efficiency.

## REFERENCES

1. Alfyorov V., Bagirov L., Dmitriev L., Feygin V., Imayev S., Lacey J. R., "Supersonic Nozzles Efficiently Separates Natural Gas Components", Oil and Gas Journal, 103, 20, (2005) 53.
2. Betting M., Volten T. V., Willink C. A. Henri J. M. and Veen M. V., *Nozzle for Supersonic Gas Flow and An Inertia Separator*, US Patent 6513345 (Feb 2003)
3. Estela J. F., Uribe, Ball S. J. and Trusler J. P. M., "Thermodynamic Properties of Gases and Liquids Determined from the Speed of Sound", created on 27 Aug 2007. Retrieved from [www3.imperial.ac.uk/portal/pls/portallive/docs/1/4651920.PDF](http://www3.imperial.ac.uk/portal/pls/portallive/docs/1/4651920.PDF) on 3 Apr 2009
4. Guo B. and Ghalambor A., *Natural Gas Engineering Handbook*, Gulf Publishing Company, 2005.
5. Karimi A., M.Abedinzadegan Abdi, "Selective removal of water from supercritical natural gas", SPE 100442, in: *Proceedings of 2006 SPE Gas Technology Symposium: Mature Fields to New Frontiers*, Calgary, Alberta, Canada, May 15–18, 2006, pp. 259–265.
6. Karimi A., M.Abedinzadegan Abdi, "Selective dehydration of high-pressure natural gas using supersonic nozzles", *Chemical Engineering and Processing: Process Intensification*, Elsevier B.V. (2008), pp. 560-568.
7. Kolass, Friedrichsdorf & Parker, *Moisture Measurement in Natural Gas*, Mitchell Instruments. Retrieved from [www.icweb.com.au/Analyzer/MoistMeas/Advantica%20Moisture%20Measurement%20Paper.doc](http://www.icweb.com.au/Analyzer/MoistMeas/Advantica%20Moisture%20Measurement%20Paper.doc) on 4<sup>th</sup> March 2009
8. Perry A. Fischer, "Subsea production systems progressing quickly", *World Oil Magazine*, Vol. 225 No. 11, Nov 2004
9. Peter S. and Hugh D. E., *Supersonic Gas Conditioning – Commercialization of Twister™ Technology*, GPA 2008 Annual Conference, Texas, USA, March 2-5 2008.

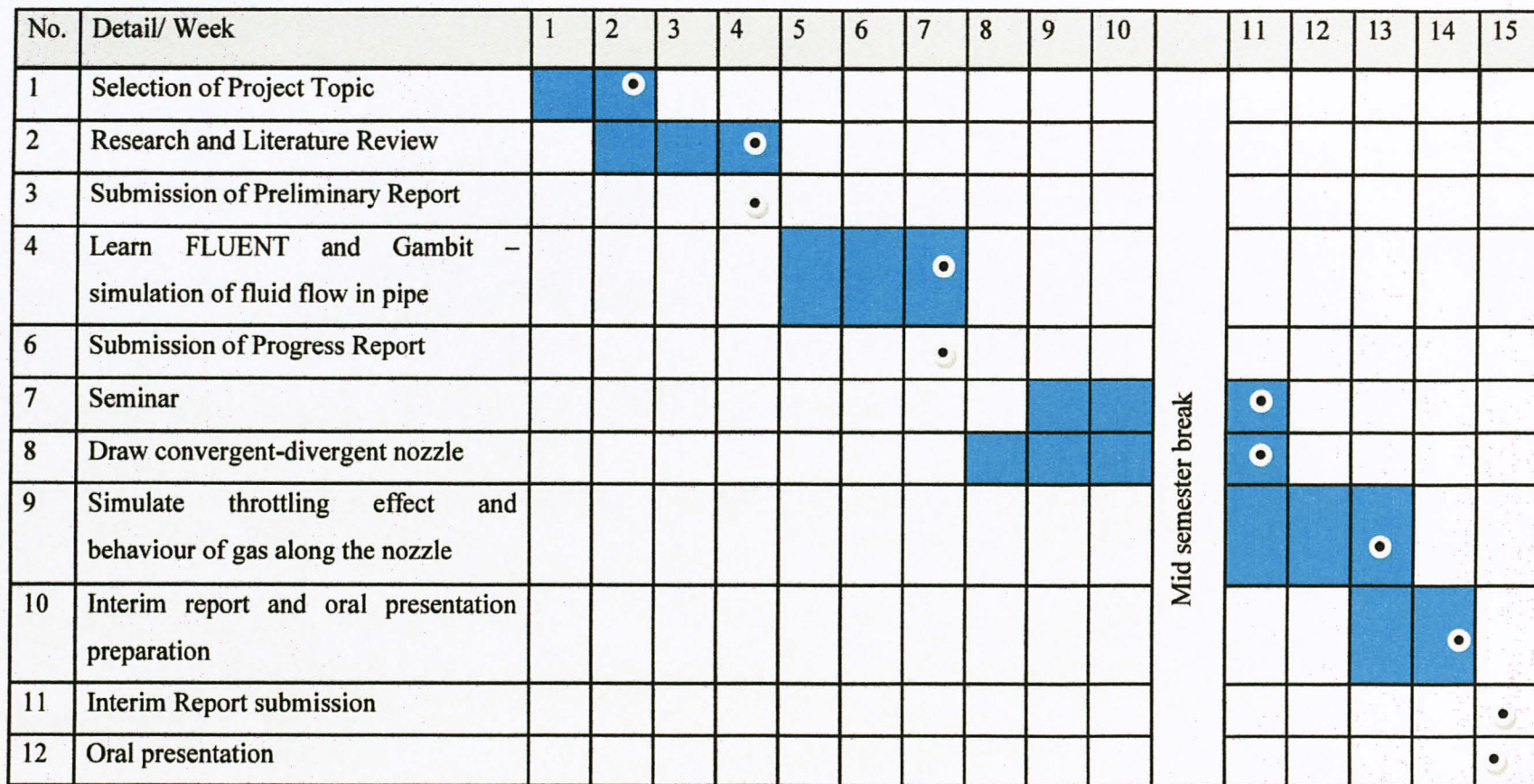


10. Speight J. G., Natural Gas - A Basic Handbook, Gulf Publishing Company, 2007, pp. 131-160
11. Unknown author, "Twister application hints at subsea separation", Offshore Magazine, Volume 64, Issue 6, June 2004

## **APPENDIX A**

### **GANTT CHARTS**

**Gantt Chart (FYP I)**



● Milestones



## Gantt Chart (FYP II)

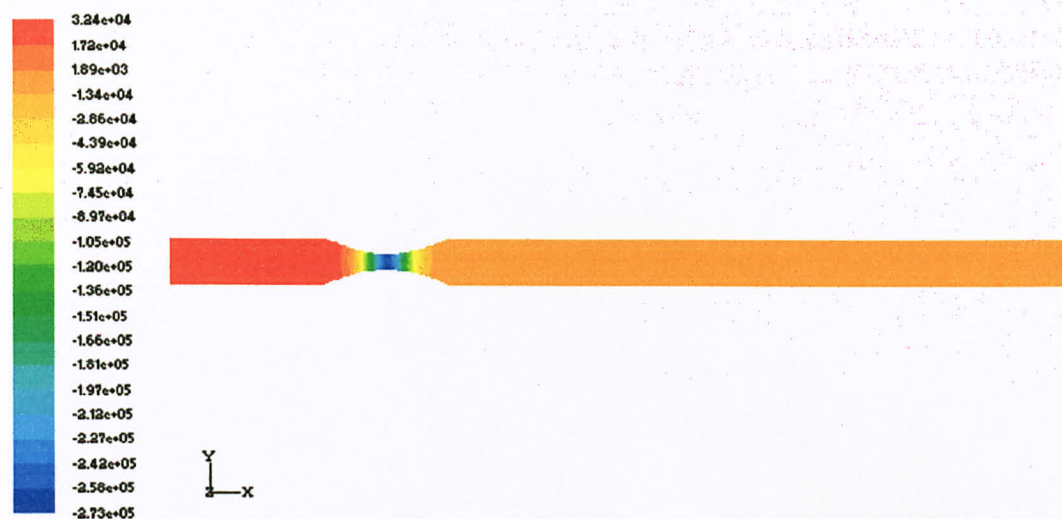
No.	Detail/ Week	1	2	3	4	5	6	7		8	9	10	11	12	13	14	15
1	Draw De Laval nozzle in 3D								Mid semester break								
2	Submission of Progress Report 1																
3	Run simulation of different parameters																
4	Submission of Progress Report 2																
5	Interpret and analyze results																
6	Poster Exhibition																
7	Documentation																
8	Submission of Dissertation (soft bound)																
9	Preparation for oral presentation																
10	Oral Presentation																
11	Submission of Project Dissertation (Hard Bound)																

• Milestone

## **APPENDIX B**

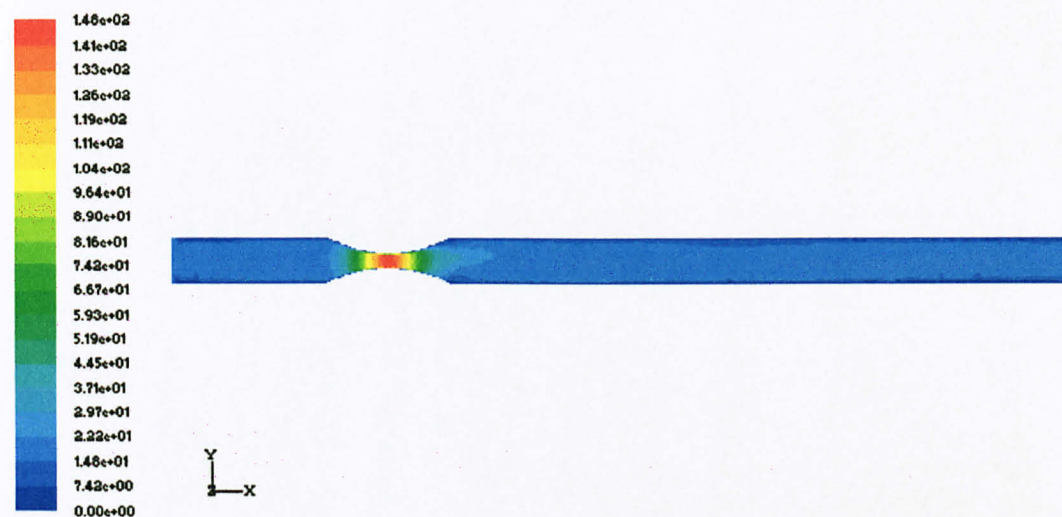
### **SIMULATION RESULT**

*Inlet mass flow rate 2kg/s*



Contours of Static Pressure (pascal)

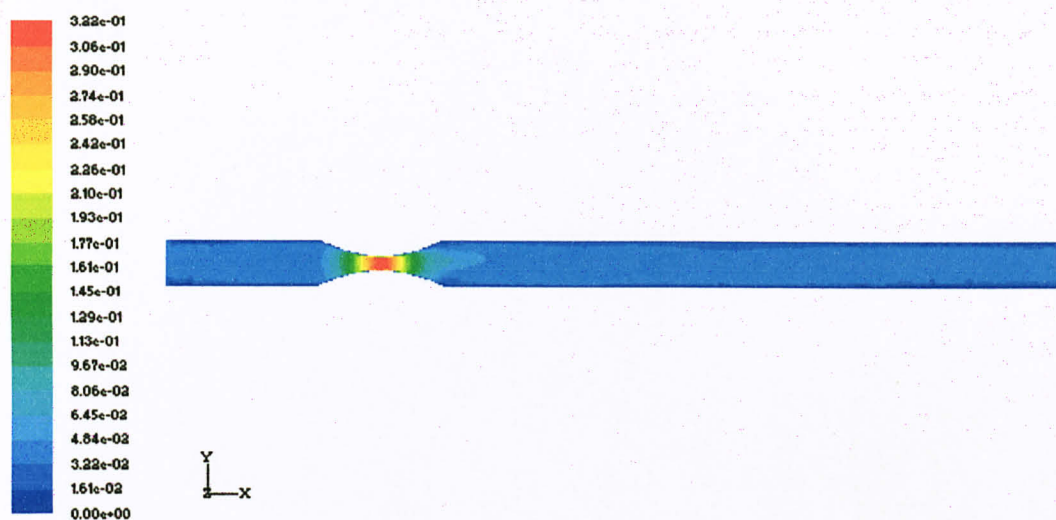
Nov 01, 2009  
FLUENT 6.2 (3d, segregated, spe, ske)



Contours of Velocity Magnitude (m/s)

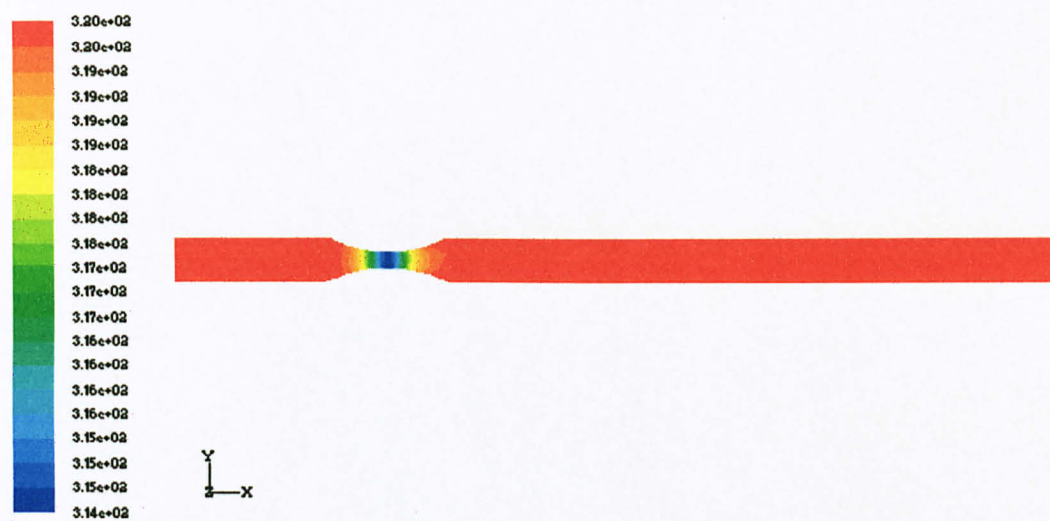
Nov 01, 2009  
FLUENT 6.2 (3d, segregated, spe, ske)





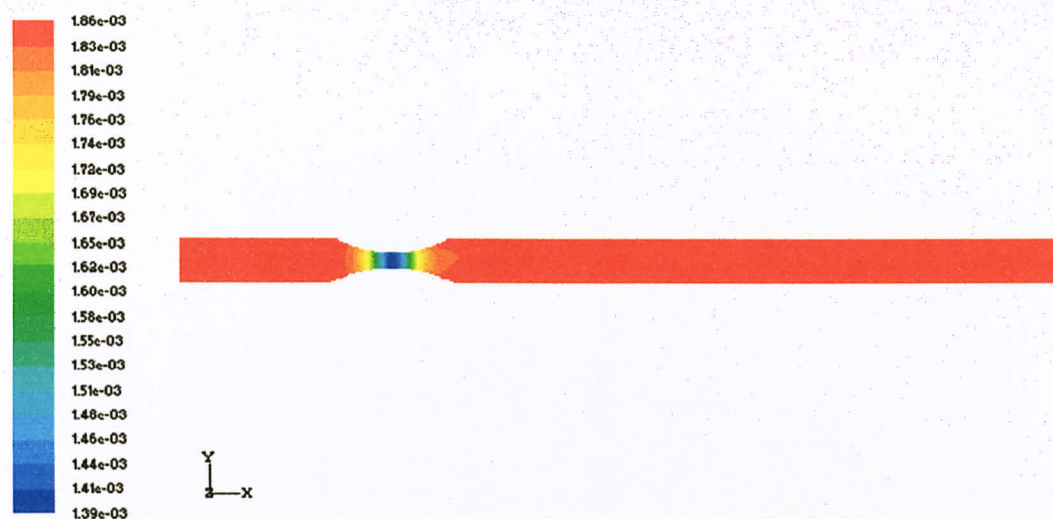
Contours of ma-number

Nov 01, 2009  
FLUENT 6.2 (3d, segregated, sse, ske)



Contours of Static Temperature (k)

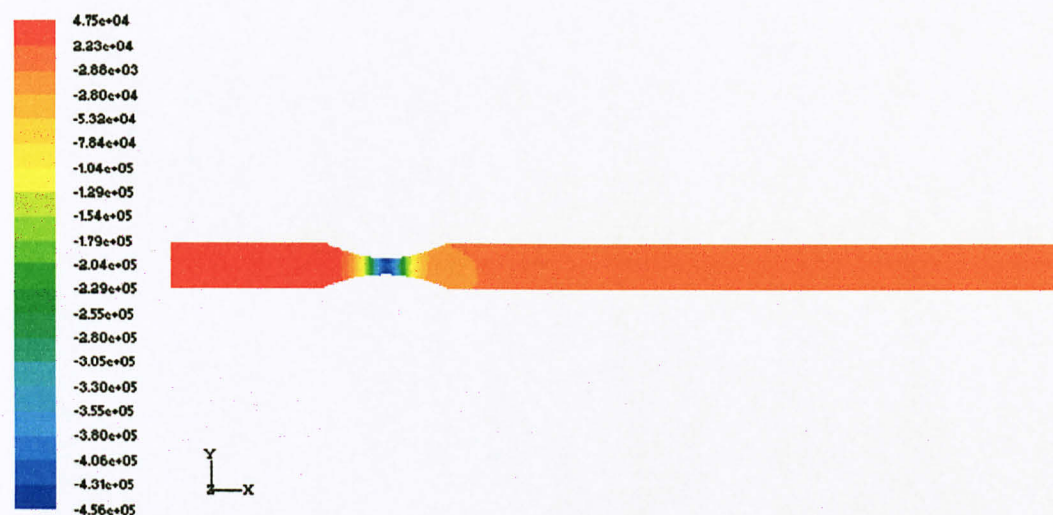
Nov 01, 2009  
FLUENT 6.2 (3d, segregated, sse, ske)



Contours of Molar Concentration of h<sub>2</sub>o (kmol/m<sup>3</sup>)

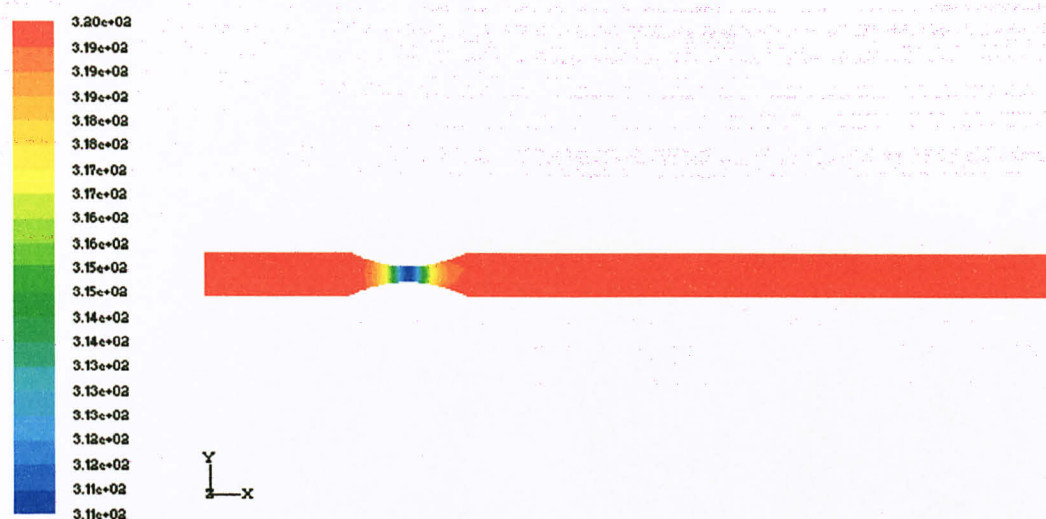
Nov 01, 2009  
FLUENT 6.2 (3d, segregated, spe, ske)

*Inlet mass flow rate 2.5kg/s*



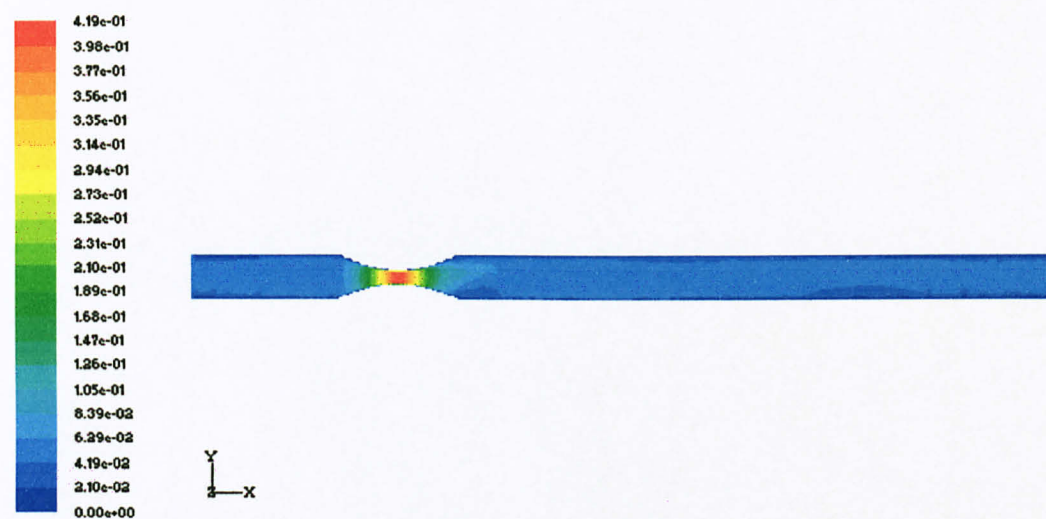
Contours of Static Pressure (pascal)

Nov 01, 2009  
FLUENT 6.2 (3d, segregated, spe, ske)



Contours of Static Temperature (K)

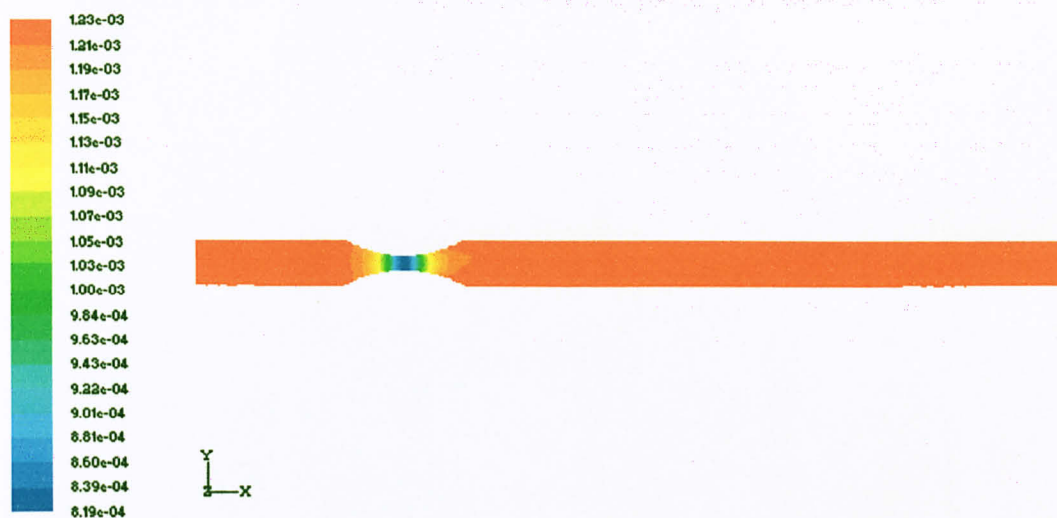
Nov 01, 2009  
FLUENT 6.2 (3d, segregated, spe, ske)



Contours of mach-number

Nov 01, 2009  
FLUENT 6.2 (3d, segregated, spe, ske)

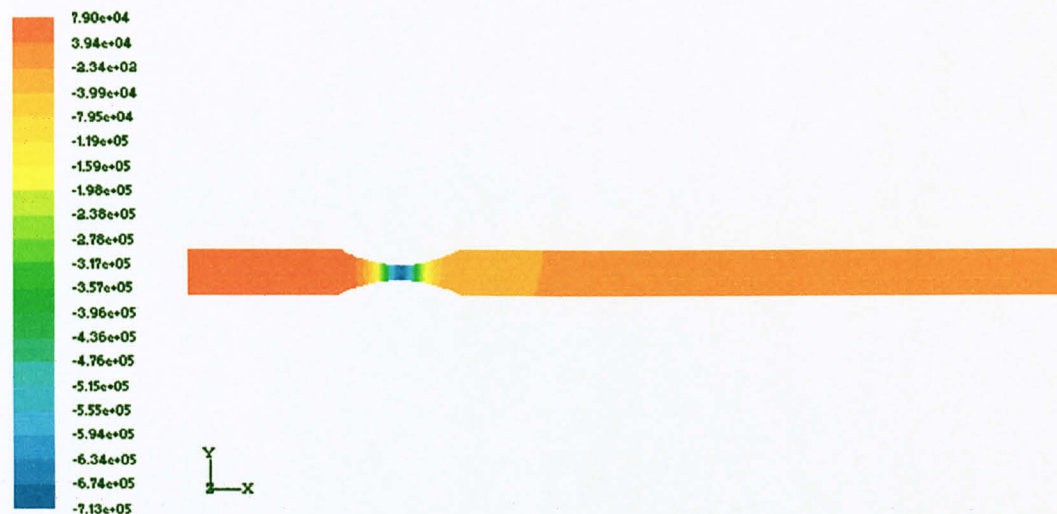




Contours of Mole fraction of h2o

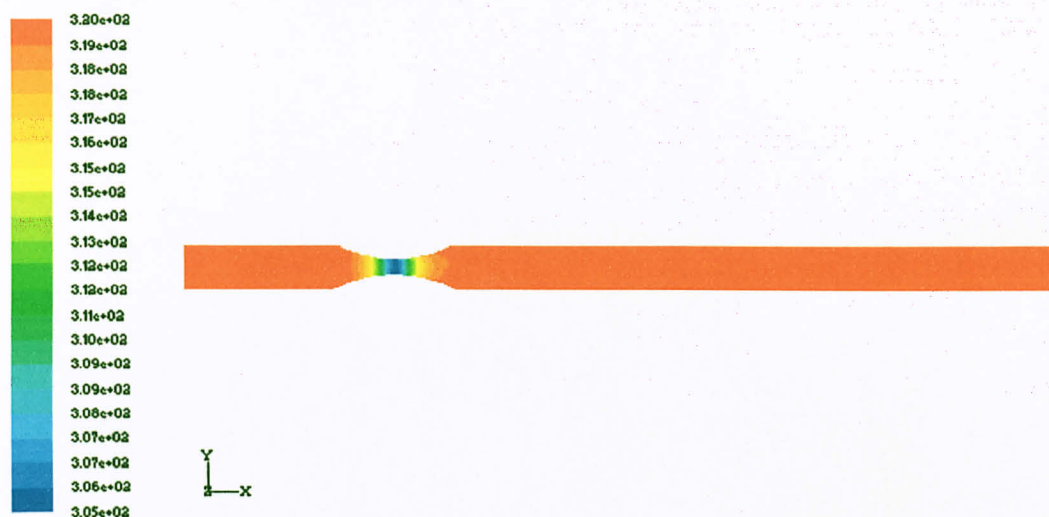
Nov 01, 2009  
FLUENT 6.2 (3d, segregated, ssc, ske)

*Inlet mass flow rate 3kg/s*



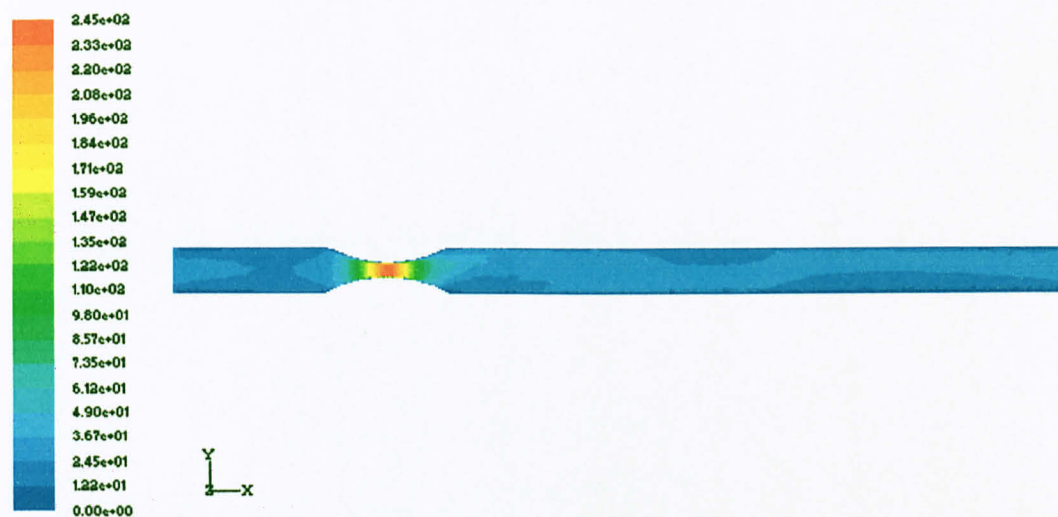
Contours of Static Pressure (pascal)

Nov 01, 2009  
FLUENT 6.2 (3d, segregated, ssc, ske)



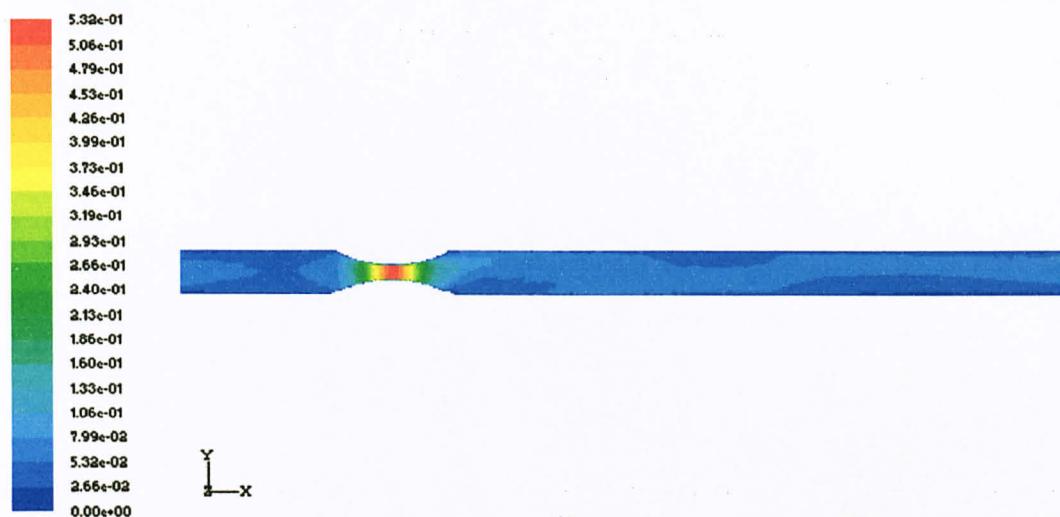
Contours of Static Temperature (K)

Nov 01, 2009  
FLUENT 6.2 (3d, segregated, cpa, ske)



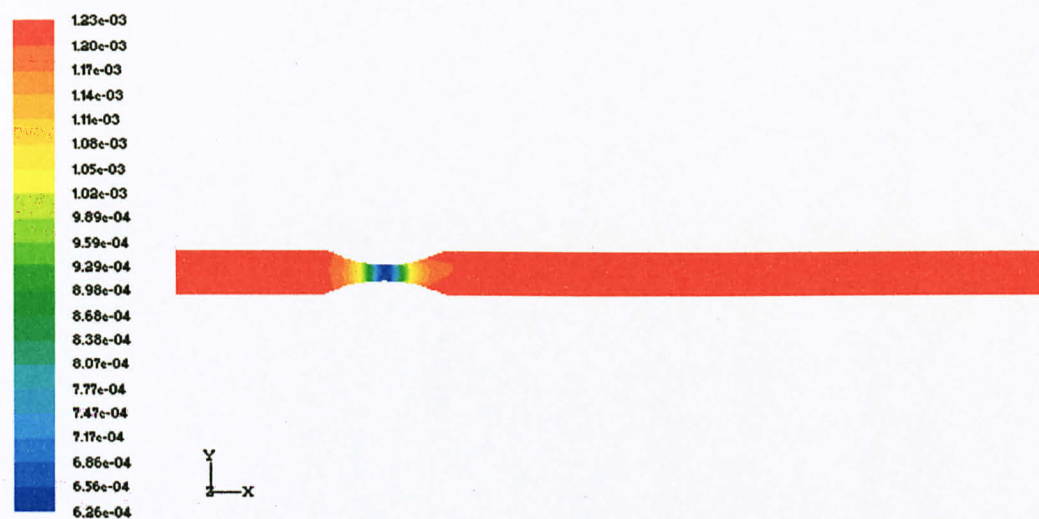
Contours of Velocity Magnitude (m/s)

Nov 01, 2009  
FLUENT 6.2 (3d, segregated, cpa, ske)



Contours of mach-number

Nov 01, 2009  
FLUENT 6.2 (3d, segregated, spe, cke)

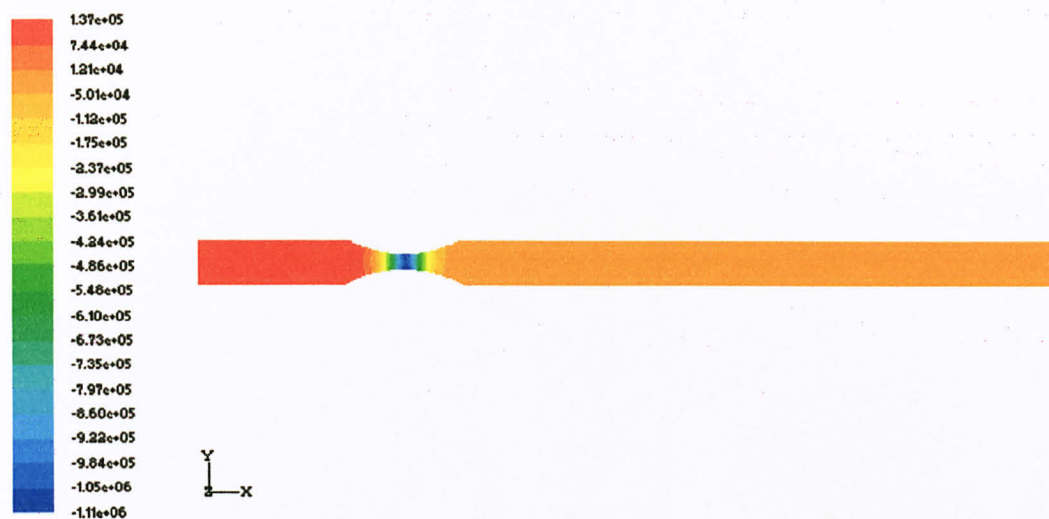


Contours of Mole fraction of H2O

Nov 01, 2009  
FLUENT 6.2 (3d, segregated, spe, cke)

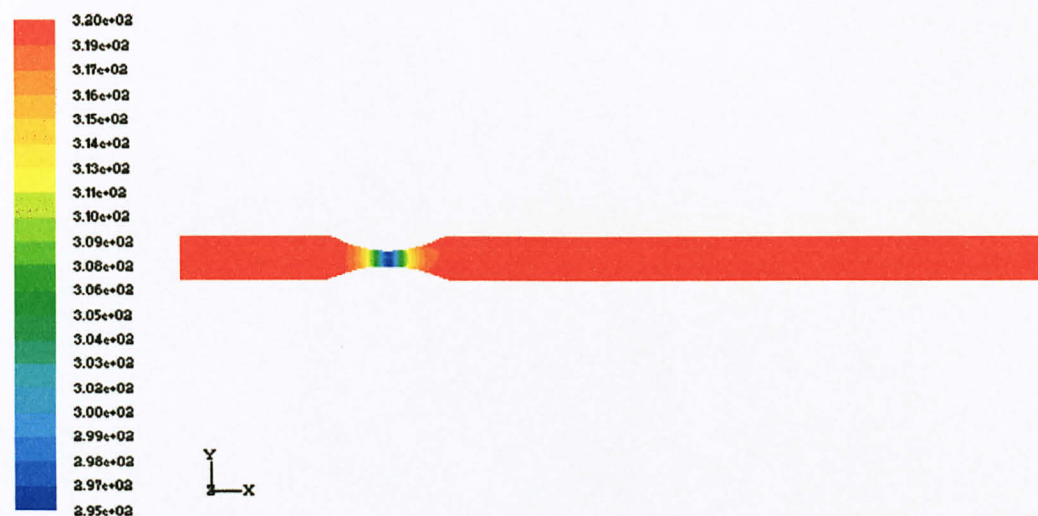


*Inlet mass flow rate 3.5kg/s*



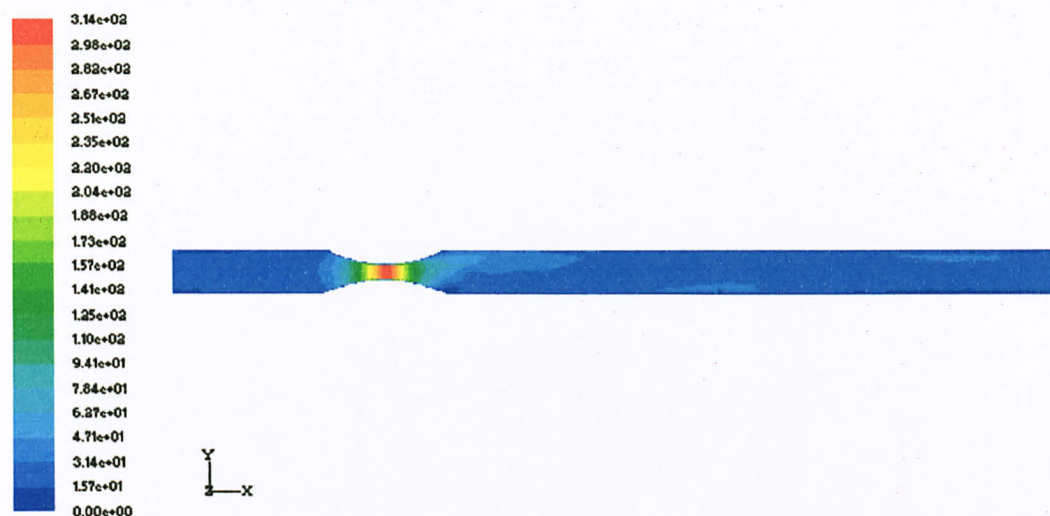
Contours of Static Pressure (pascal)

Nov 01, 2009  
FLUENT 6.2 (3d, segregated, smp, ske)



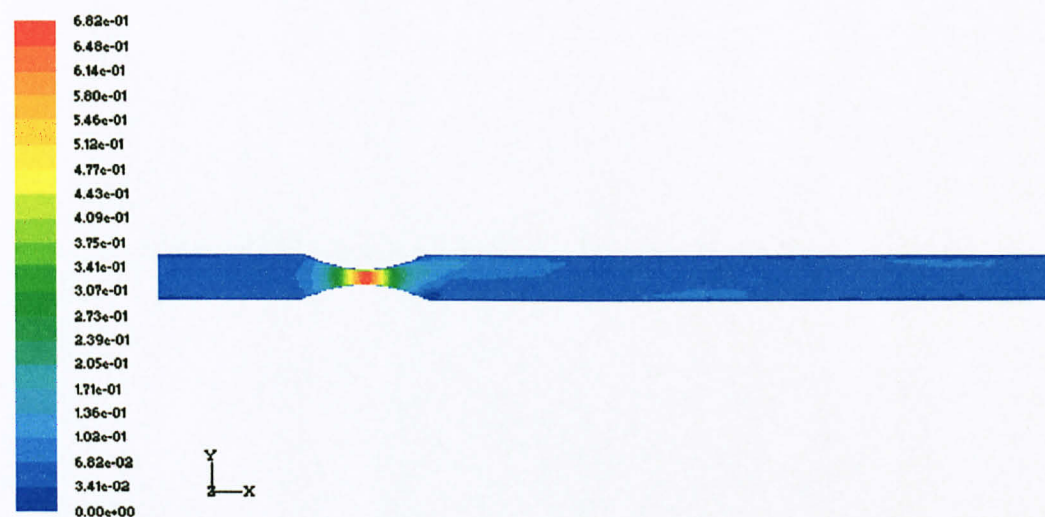
Contours of Static Temperature (K)

Nov 01, 2009  
FLUENT 6.2 (3d, segregated, smp, ske)



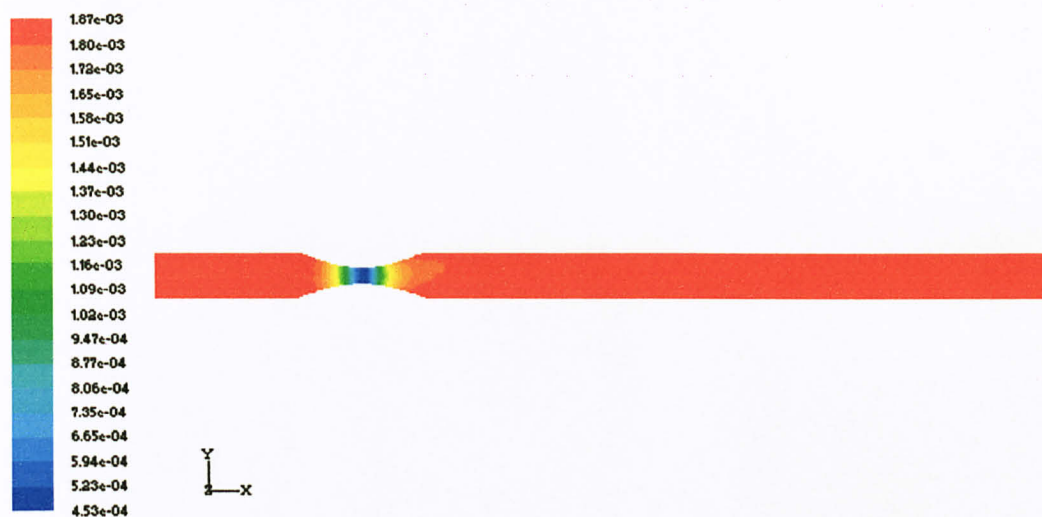
Contours of Velocity Magnitude (m/s)

Nov 01, 2009  
FLUENT 6.2 (3d, segregated, spe, ske)



Contours of mach-number

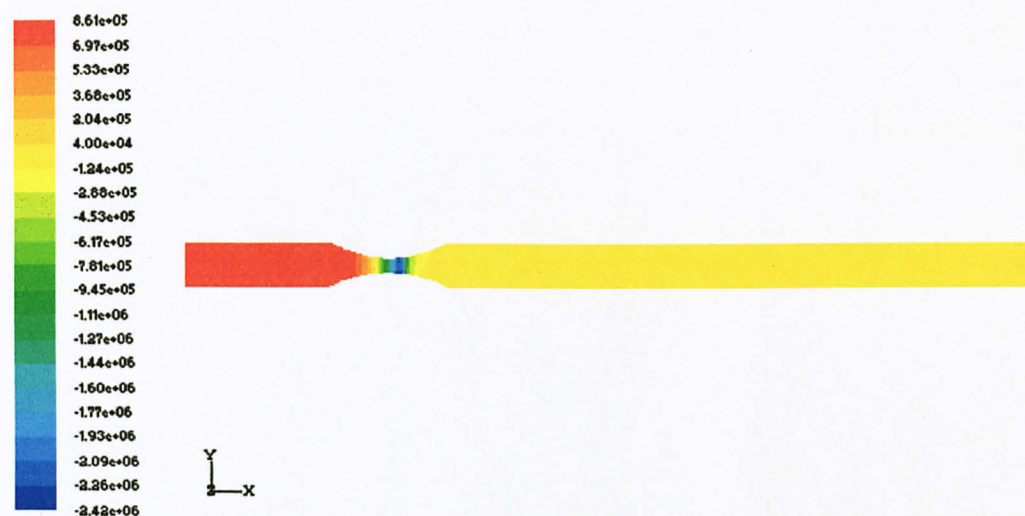
Nov 01, 2009  
FLUENT 6.2 (3d, segregated, spe, ske)



Contours of Molar Concentration of  $H_2O$  (kmol/m<sup>3</sup>)

Nov 01, 2009  
FLOENT 6.2 (3d, segregated, spe, ske)

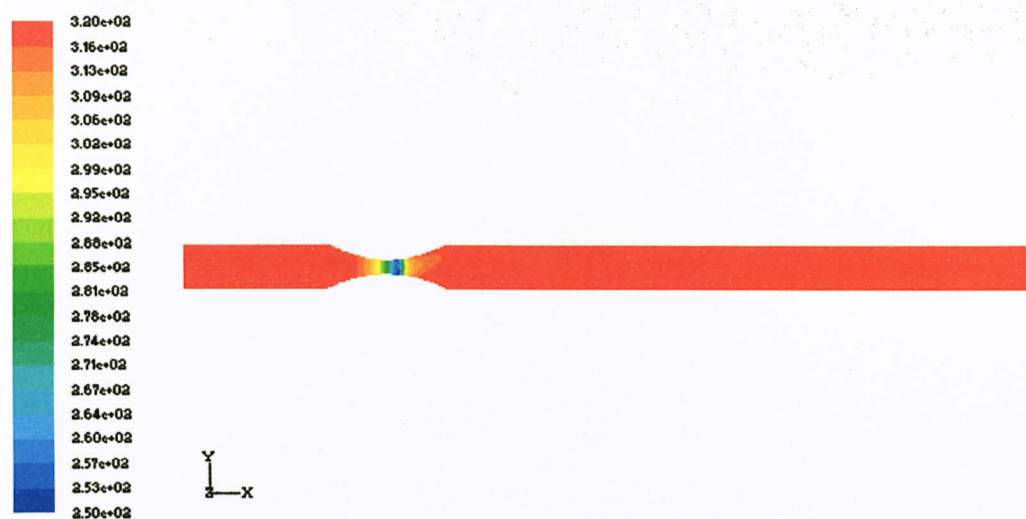
**Inlet mass flow rate 4.5kg/s**



Contours of Static Pressure (pascal)

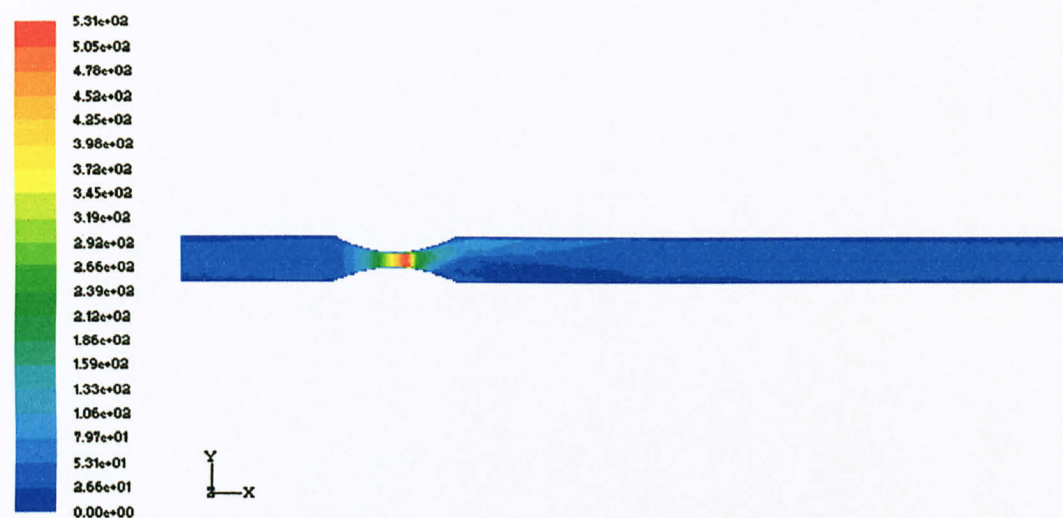
Nov 02, 2009  
FLOENT 6.2 (3d, segregated, spe, ske)





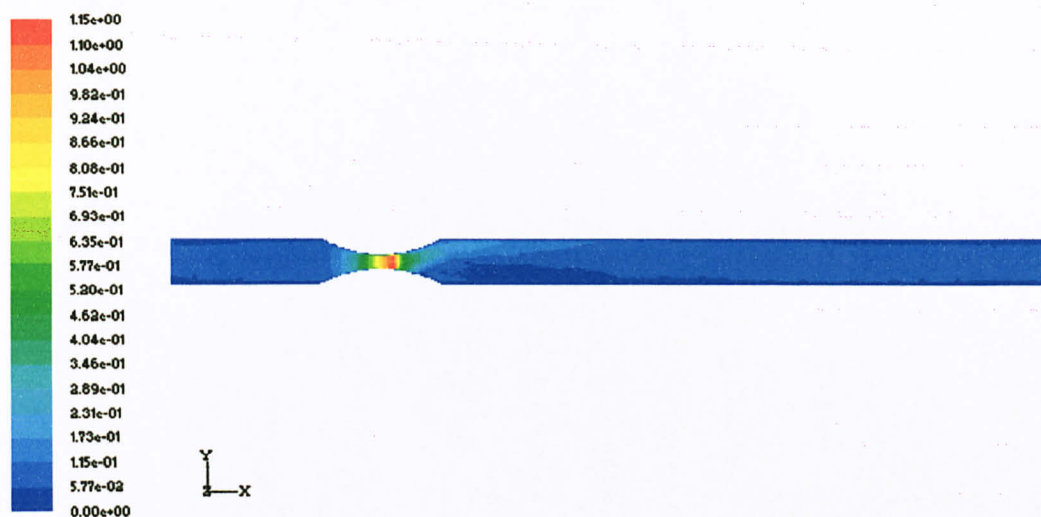
Contours of Static Temperature (K)

Nov 02, 2009  
FLUENT 6.2 (3d, segregated, cpa, cke)



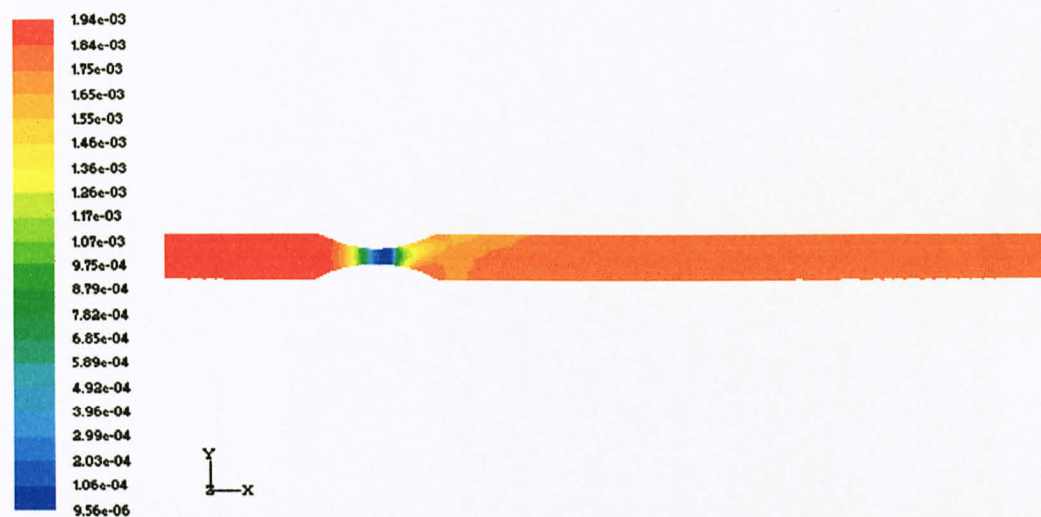
Contours of Velocity Magnitude (m/s)

Nov 02, 2009  
FLUENT 6.2 (3d, segregated, cpa, cke)



Contours of mach-number

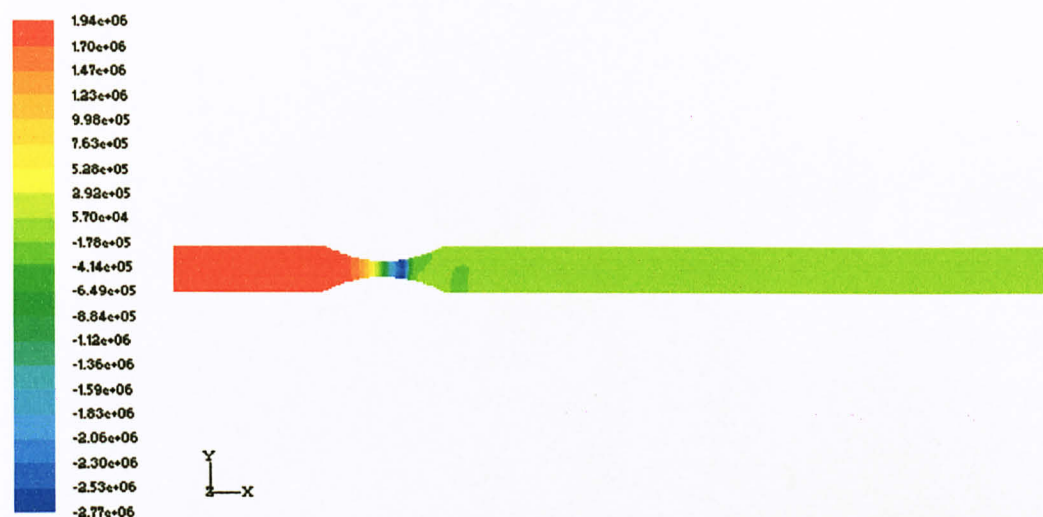
Nov 02, 2009  
 FLUENT 6.2 (3d, segregated, smp, ske)



Contours of Molar Concentration of h2o (kmol/m3)

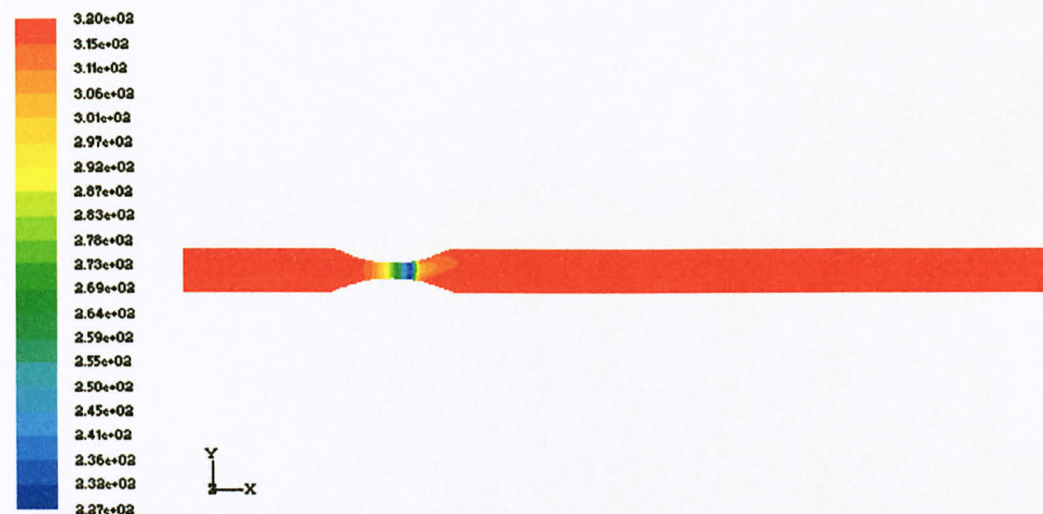
Nov 02, 2009  
 FLUENT 6.2 (3d, segregated, smp, ske)

*Inlet mass flow rate 5.5kg/s*



Contours of Static Pressure (pascal)

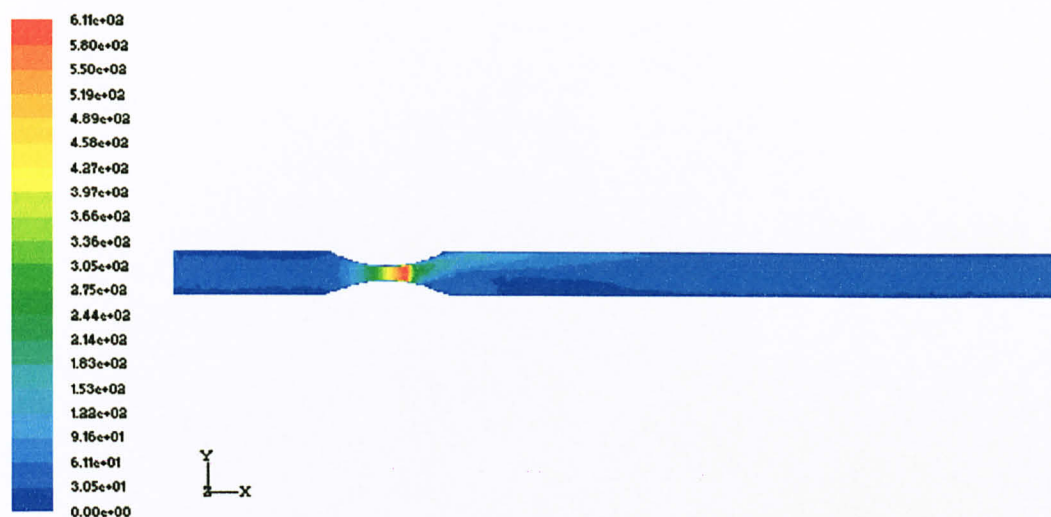
Nov 02, 2009  
FLUENT 6.2 (3d, segregated, spc, ske)



Contours of Static Temperature (K)

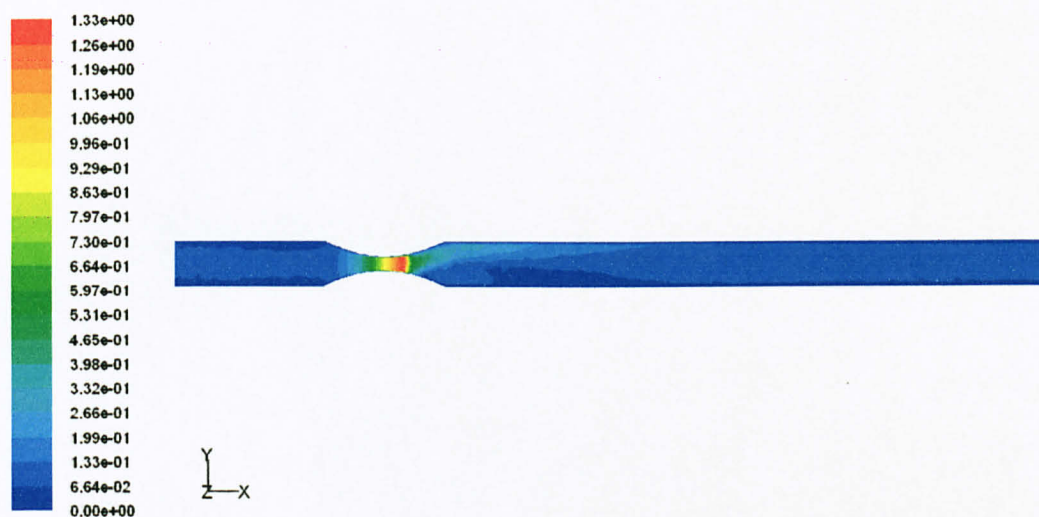
Nov 02, 2009  
FLUENT 6.2 (3d, segregated, spc, ske)





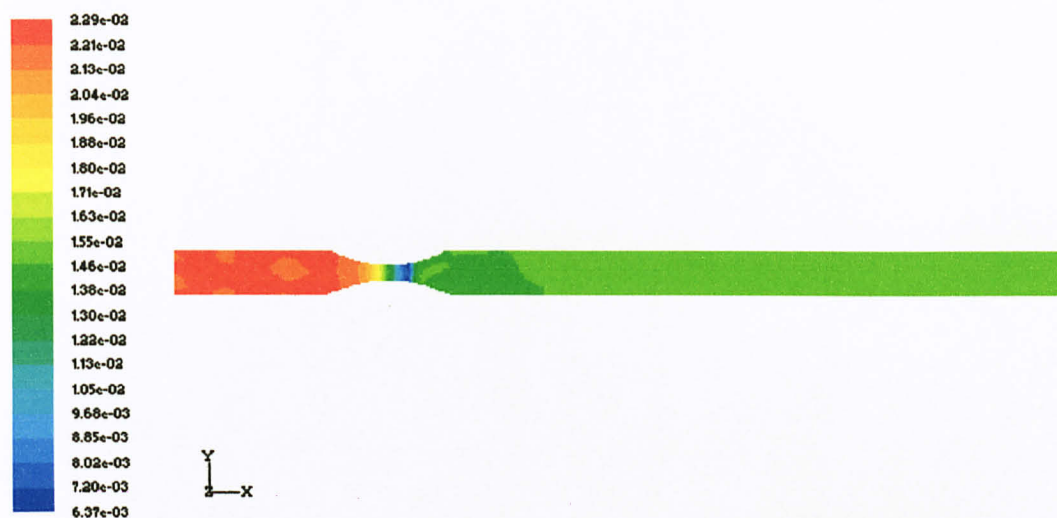
Contours of Velocity Magnitude (m/s)

Nov 02, 2009  
FLUENT 6.2 (3d, segregated, mpe, ske)



Contours of mach-number

Nov 29, 2009  
FLUENT 6.2 (3d, segregated, spe, ske)



Contours of Molar Concentration of H<sub>2</sub>O (kmol/m<sup>3</sup>)

Nov 02, 2009  
FLUENT 6.2 (3d, segregated, sps, cke)

## **APPENDIX C**

### **SIMULATION RESULT VALIDATION DATA**



**Table C1: Comparison of experimental and simulation result**

<b>Experimental</b>		<b>Simulation</b>	
<b>Temperature difference (K)</b>	<b>Pressure ratio, P1/P2</b>	<b>Temperature difference (K)</b>	<b>Pressure ratio, P1/P2</b>
0	1	6	1.2292
10	1.2344	9	1.2519
20	1.4375	15	1.3441
30	1.6094	25	1.4728
40	1.7969	47	1.8558
50	1.9688	70	2.5745
60	2.1563	84	3.5533
70	2.4375	93	5.4264